Supplementary material related to

Feasibility of phosphoproteomics on leftover samples after RNA extraction with guanidinium thiocyanate

Frank Rolfs[a,b,c], Sander R. Piersma[a], Mariana Paes Dias[b,c], Jos Jonkers[b,c*], Connie R. Jimenez[a,*]

[a] *Amsterdam UMC, OncoProteomics Laboratory, Department Medical Oncology, location VUmc, Amsterdam, The Netherlands*
[b] *Division of Molecular Pathology, The Netherlands Cancer Institute, Amsterdam, The Netherlands*
[c] *Oncode institute, Amsterdam, The Netherlands*
** Joint corresponding authors: j.jonkers@nki.nl & c.jimenez@amsterdamumc.nl*

Supplementary Figures 1-29 & legend
Supplementary Table 1 legend
Supplementary Table 2 legend

overview figures		**MBR-on**			**MBR-off**	
	U2OS	**mouse**	**human**	**U2OS**	**mouse**	**human**
main figure	**F1**			S5		
main figure		**F2**	**F2**		S19	S19
total number PS, percentage MVs, boxplots normalized data	S1	S11	S14	S6	S20	S24
overlap class 1 PS % & class all, GO unique genes urea, RNAB	S2	S12	S15	S7	S21	S25
U2OS PTM-SEA signatures	S3			S8		
pTyr sites in dataset	S4	S13	S16-18	S9	S22	S26-28
correlation urea MBR-on/off; RNAB MBR-on/off	*S10*	*S23*	*S29*	*S10*	*S23*	*S29*

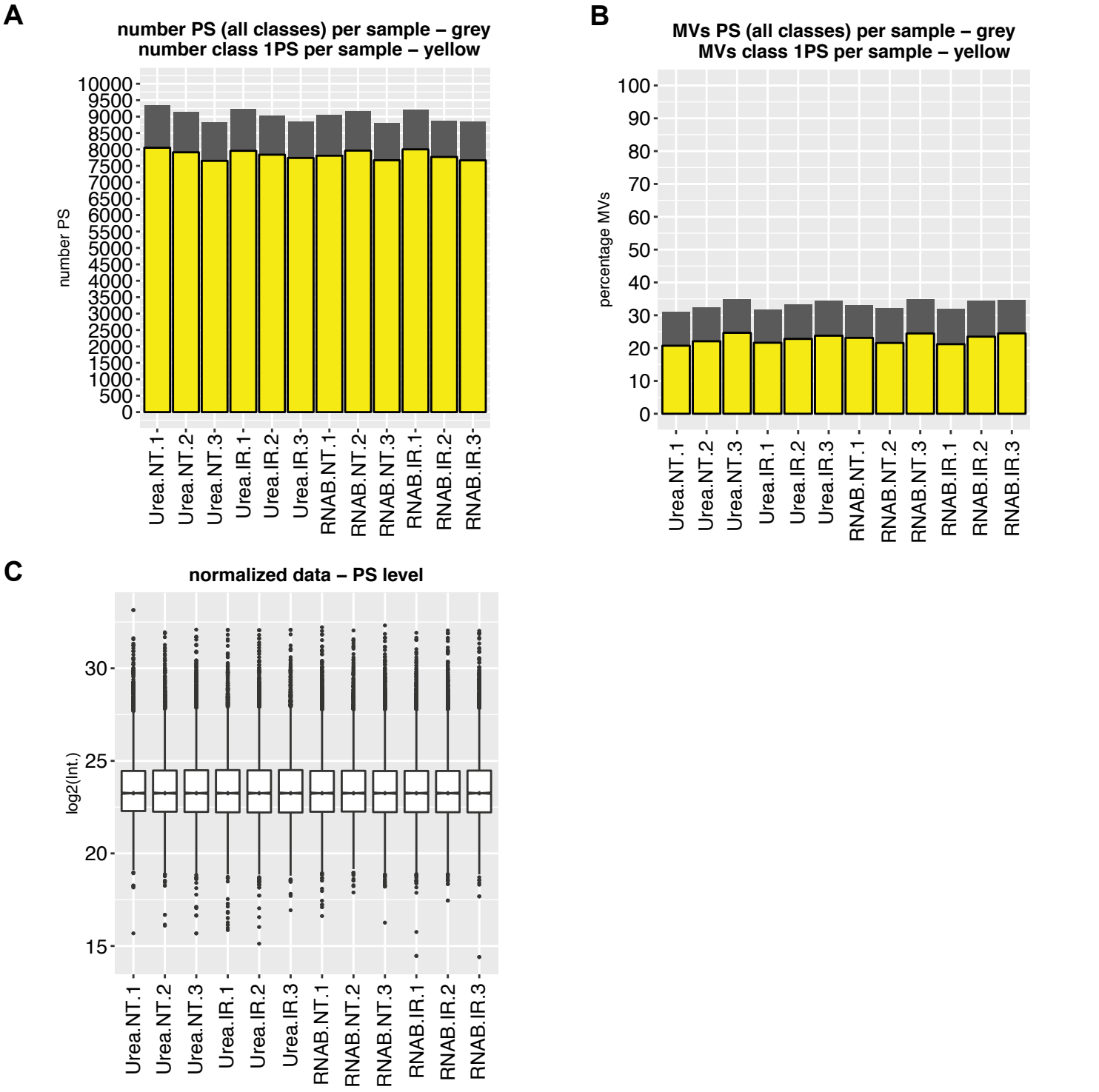

Supplementary Figure 1: Phosphoproteomic profiling of U2OS cells after irradiation or without treatment and lysis with urea or RNA-Bee (RNAB).
A) Bar graph depicting the number of identified phosphosites (PS) per sample. Grey color indicates all classes of identified PS. Yellow color marks the number of class 1 PS which have a localization probability ≥ 0.75.
B) Bar graph showing the percentage of missing values (MV) per sample. In a data matrix of the entire experiment, MV are situations of not detected PS for a given sample which were identified in at least one of samples in the matrix.
C) Phosphosite level box plot showing normalized data for each sample. The graph is based on PS of all classes.
For supplementary Fig. 1 A-C MaxQuant MBR option was enabled for all samples.

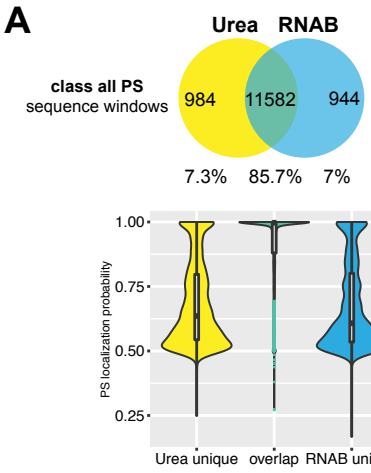

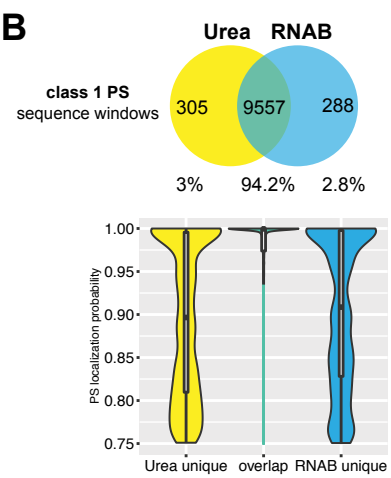

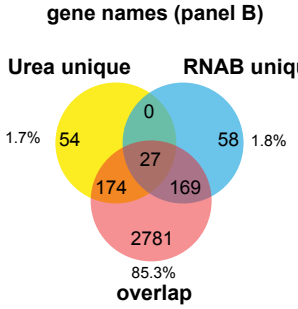

GO analysis: BP for Urea unique gene names (54)
- regulation of receptor recycling [AP1AR, CHMP5, KIF16B]
- regulation of spindle assembly [CHMP5, SMC3, SPAG5]

GO analysis: BP for RNAB unique gene names (58)
- no significant GO-terms found

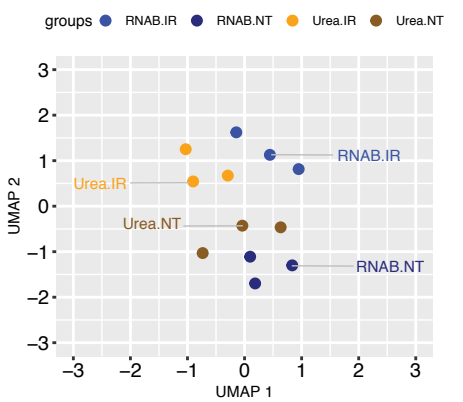

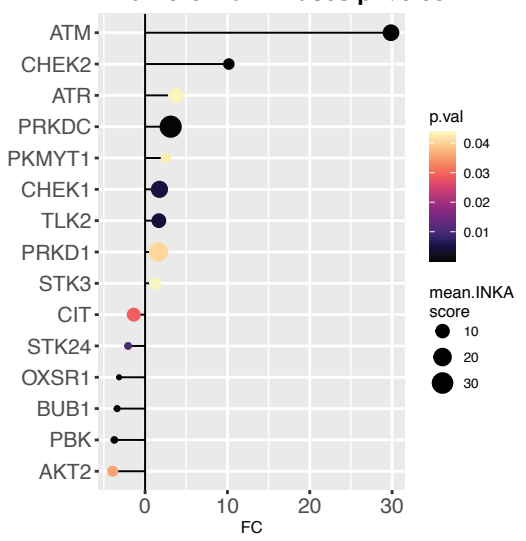

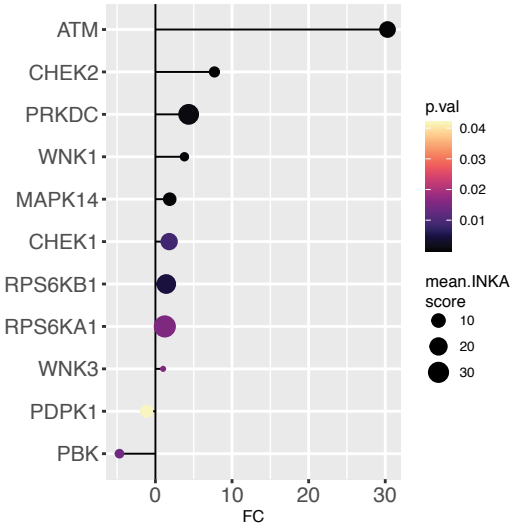

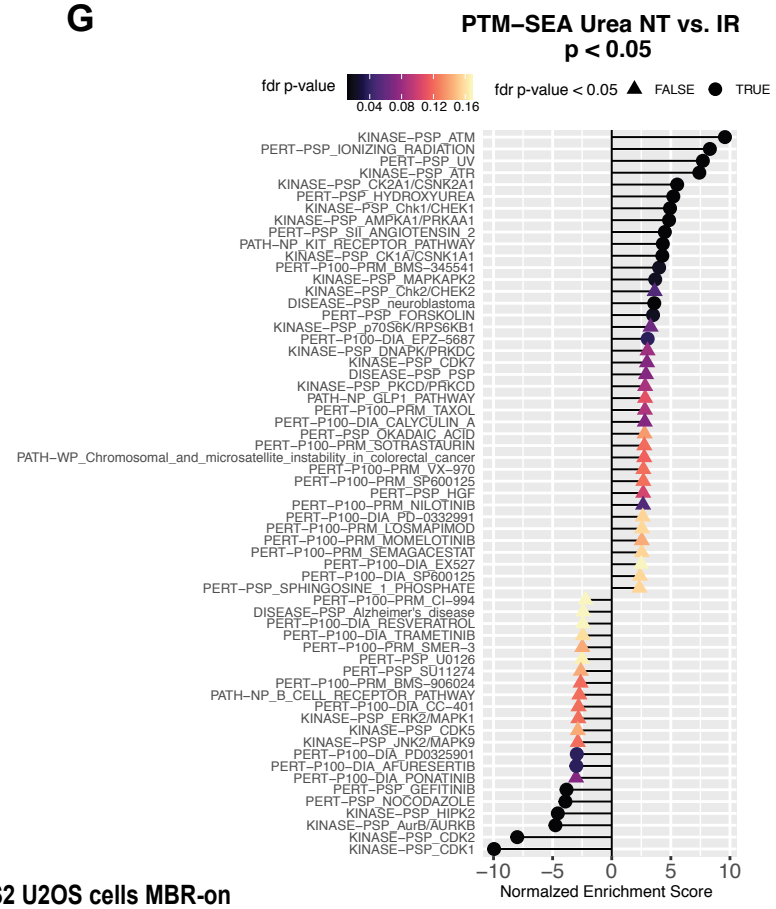

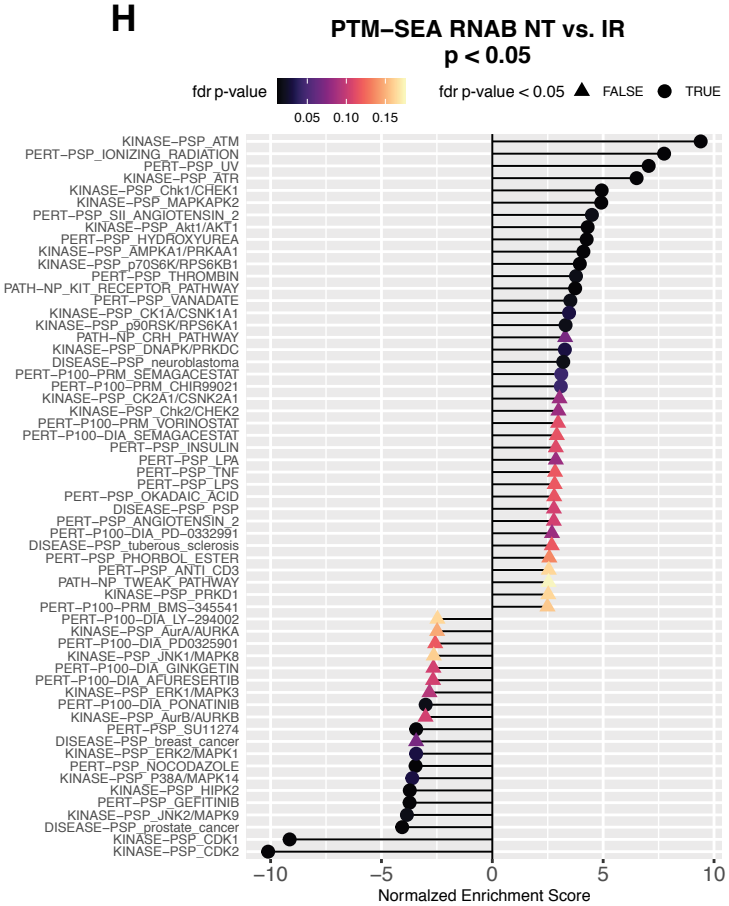

S2 U2OS cells MBR-on

Supplementary Figure 2: U2OS cells: Overlay of phosphosites identified per isolation method, kinase activity and phosphosite signatures after irradiation of urea and RNA-Bee (RNAB) lysed cells.
A) Related to Fig. 1 B. Upper Venn diagram showing overlap of class all detected phosphosites (PS) between urea and RNAB isolated samples. Sequence windows of identified PS were used. Lower violin plot illustrating localization probability distribution of PS compared in upper Venn diagram. In general, shared PS showed higher localization probability than isolation method unique PS.
B) Related to Fig. 1 B. Same as supplementary Fig. 2 A for class 1 phosphosites.
C) Related to Fig. 1 B. Upper Venn diagram showing shared gene names of phosphorylated proteins shown in supplementary Fig. 2 B. Lower part showing the result of gene ontology (GO) enrichment analysis for isolation method unique gene names using biological process (BP) terms.
D) Related to Fig. 1 C. UMAP embedding of class 1 phosphosite data.
E) Related to Fig. 1 D. Single sample inferred kinase activity (INKA) analysis was performed to detect activated kinases for urea lysed cells. Comparing untreated (NT) vs. irradiated (IR) samples, differential INKA scores were then detected using limma. Fold changes of significant kinases found are plotted. Significance is color coded. INKA score magnitude is indicated via circle size and shows the average INKA scores of three samples with the same treatment and isolation method.
F) Same as E for RNAB lysed cells.
G) Related to Fig. 1 E. Phosphosite specific signature analysis (PTM-SEA) was performed using PS of urea lysed cells and comparing untreated (NT) vs. irradiated (IR) samples. Bar plot shows normalized enrichment scores (NES) for detected, significant signatures. Adjusted p-value is color and shape coded.
H) Same as G for RNAB lysed cells.
For supplementary Fig. 2 A-H MaxQuant MBR option was enabled for all samples.

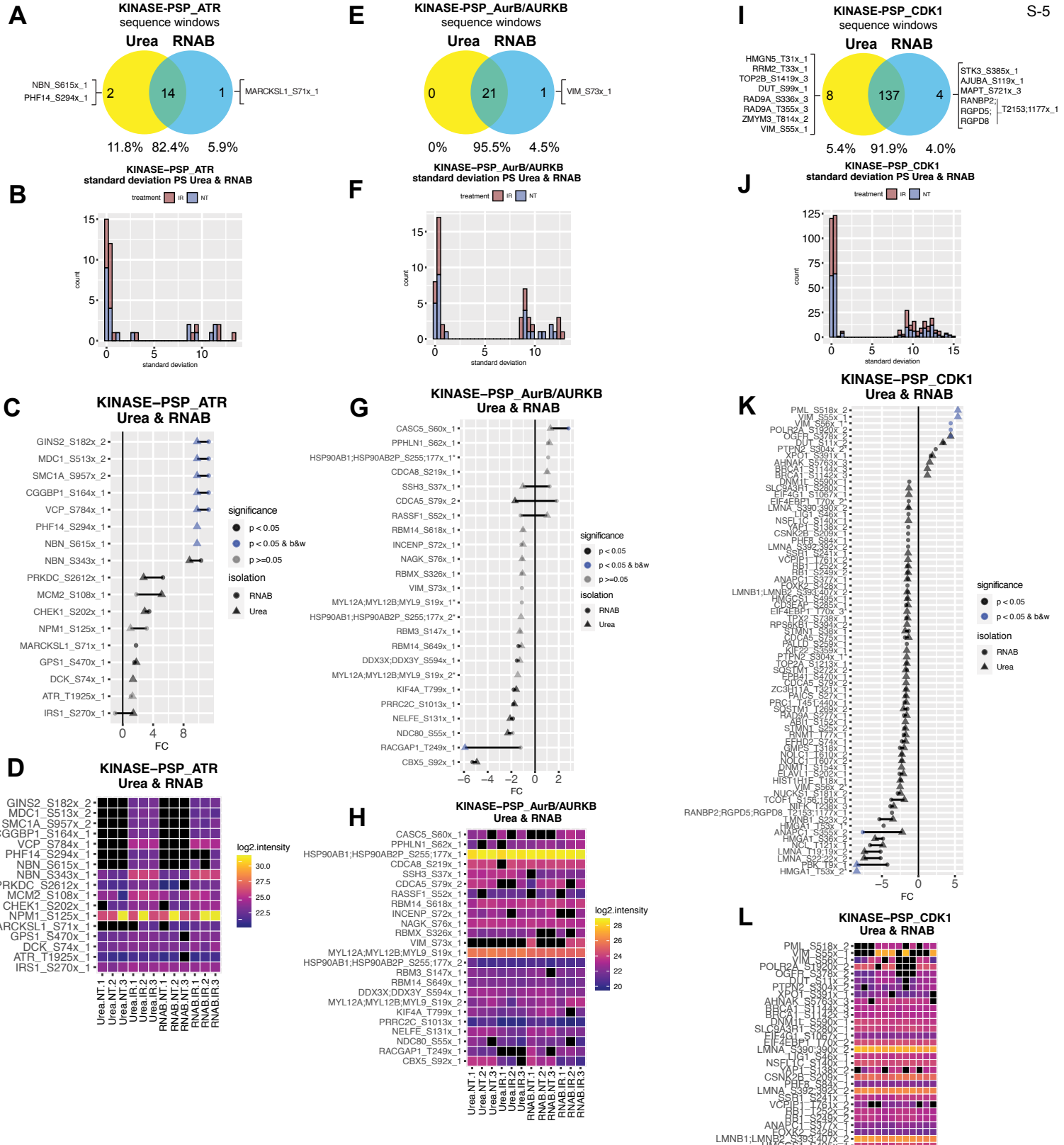

Supplementary Figure 3: U2OS cells: Similarity of selected PTM-SEA signatures derived from comparison of untreated vs. irradiated urea and RNA-Bee (RNAB) lysed cells.

A-L) Same as Fig. 1 F-I for PTM-SEA signature KINASE-PSP_ATR (A-D), KINASE-PSP_AurB/AURKB (E-H) and KINASE-PSP_CDK1 (I-L). Note that due to the high number of signature PS for CDK1, only significant PS are depicted in K-L. For supplementary Fig. 3 A-L MaxQuant MBR option was enabled for all samples.

S3 U2OS cells MBR-on

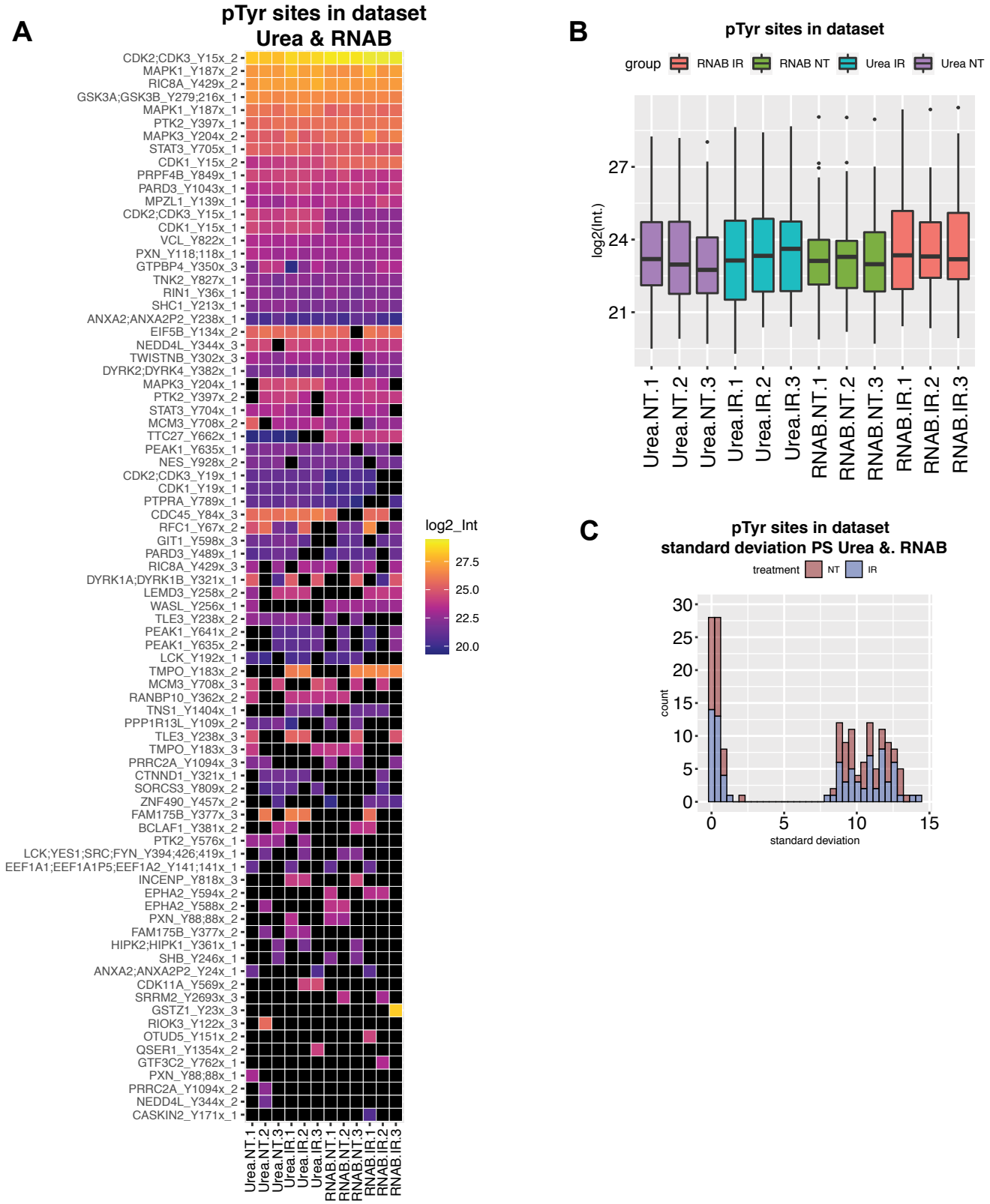

Supplementary Figure 4: U2OS cells: Comparison of pTyr sites detected in dataset.
A) Heatmap visualizing class 1 pTyr sites detected in this study. The measured log2 intensity is color coded for each PS with highest intensities on top. Black color indicates no detection. x_1, x_2, x_3 indicate if PS were derived from single or multiple phosphorylated peptides.
B) Box plot showing the combined intensities for detected class 1 pTyr sites per sample. Treatment groups and isolation methods are color coded.
C) Standard deviation was calculated over urea and RNAB sites after irradiation (IR) or no treatment (NT). The resulting frequency distribution for class 1 pTyr sites in the dataset is plotted.
For supplementary Fig. 4 A-C MaxQuant MBR option was enabled for all samples.

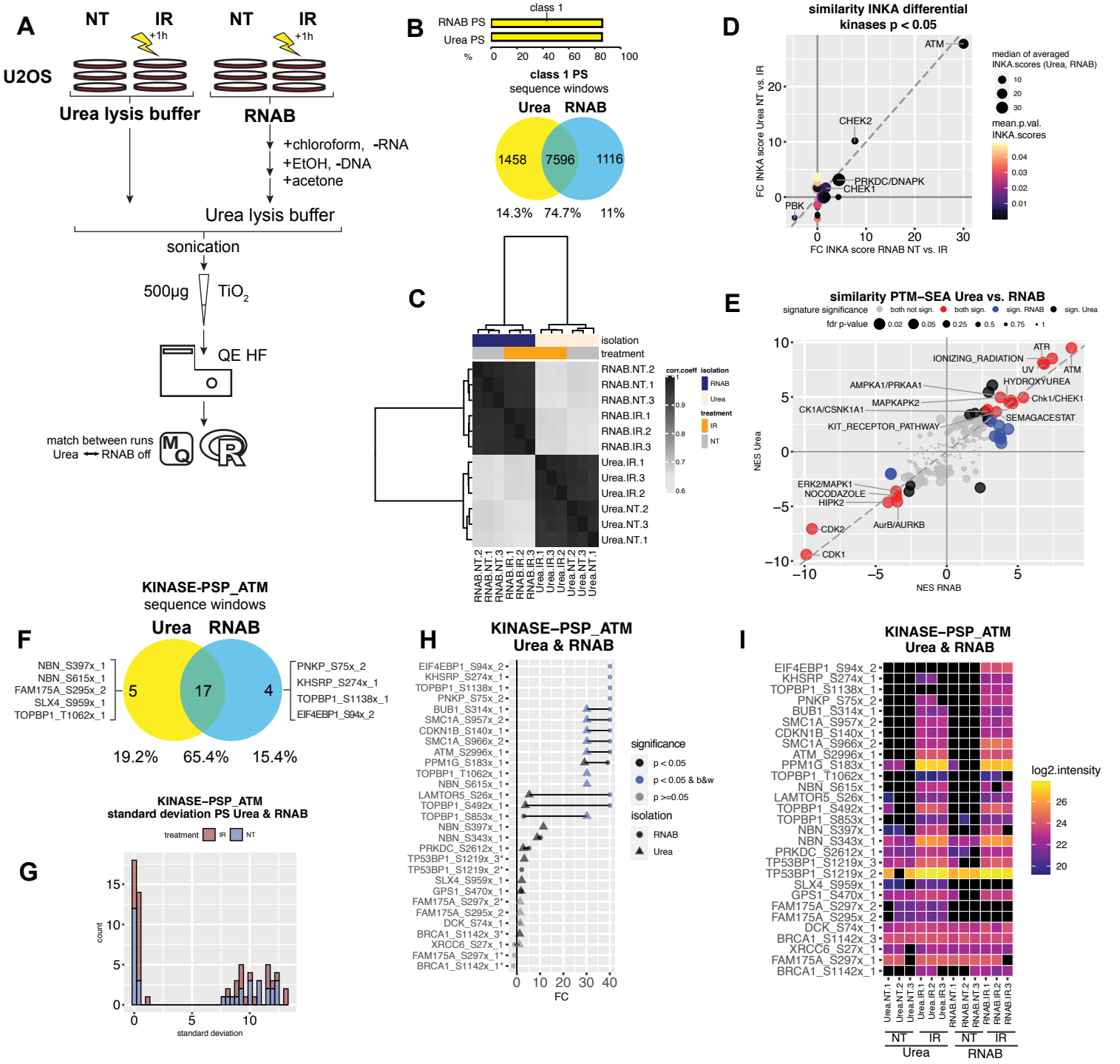

Supplementary Figure 5: Phosphoproteomic data comparison of untreated and irradiated U2OS cells extracted with urea lysis buffer or RNA-Bee shows very high similarity.
A-I) Same as Fig. 1. Urea and RNAB isolated samples were searched separately, i.e. with MaxQuant MBR option disabled between urea and RNAB isolated samples but enabled for samples inside the same isolation group.

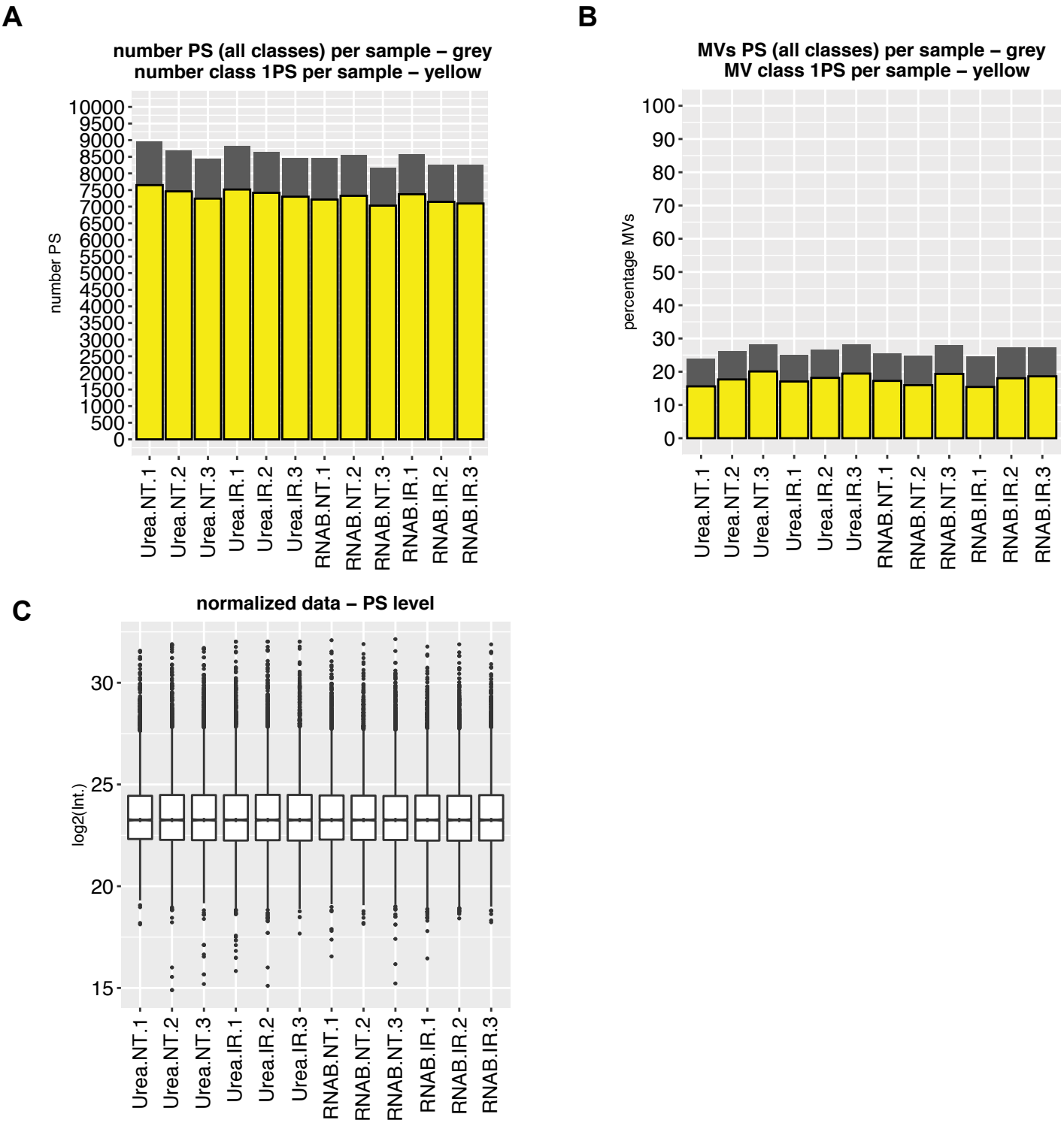

Supplementary Figure 6: U2OS cells: Phosphoproteomic profiling cells after irradiation or without treatment and lysis with urea or RNA-Bee (RNAB).
A-C) Same as supplementary Fig. 1. Urea and RNAB isolated samples were searched separately, i.e. with MaxQuant MBR option disabled between urea and RNAB isolated samples but enabled for samples inside the same isolation group.

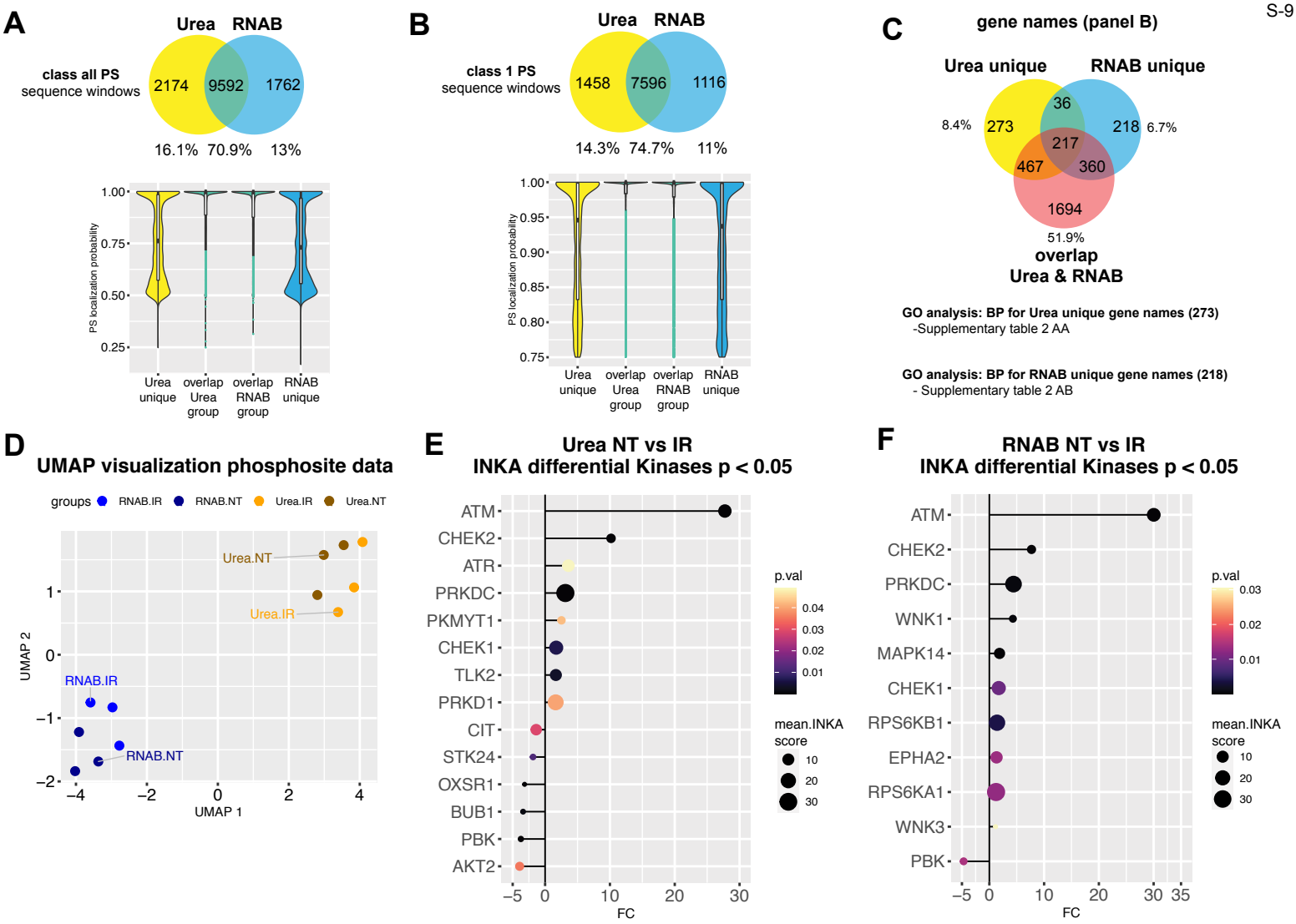

S7 U2OS cells MBR-off

Supplementary Figure 7: U2OS cells: Overlay of phosphosites identified per isolation method, kinase activity and phosphosite signatures after irradiation of urea and RNA-Bee (RNAB) lysed cells.
A-H) Same as in supplementary Fig. 2. Urea and RNAB isolated samples were searched separately, i.e. with MaxQuant MBR option disabled between urea and RNAB isolated samples but enabled for samples inside the same isolation group.

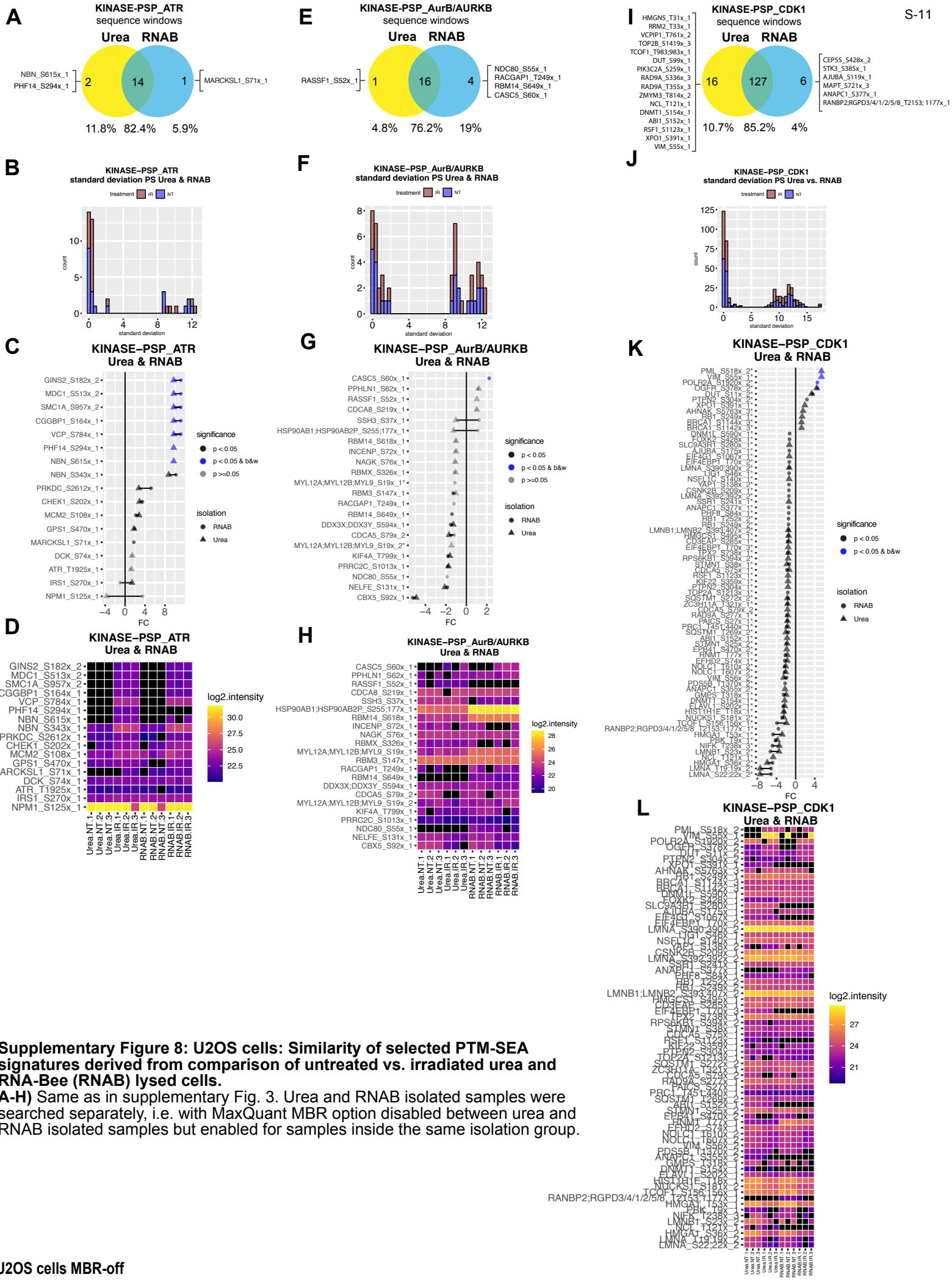

Supplementary Figure 8: U2OS cells: Similarity of selected PTM-SEA signatures derived from comparison of untreated vs. irradiated urea and RNA-Bee (RNAB) lysed cells.

A-H) Same as in supplementary Fig. 3. Urea and RNAB isolated samples were searched separately, i.e. with MaxQuant MBR option disabled between urea and RNAB isolated samples but enabled for samples inside the same isolation group.

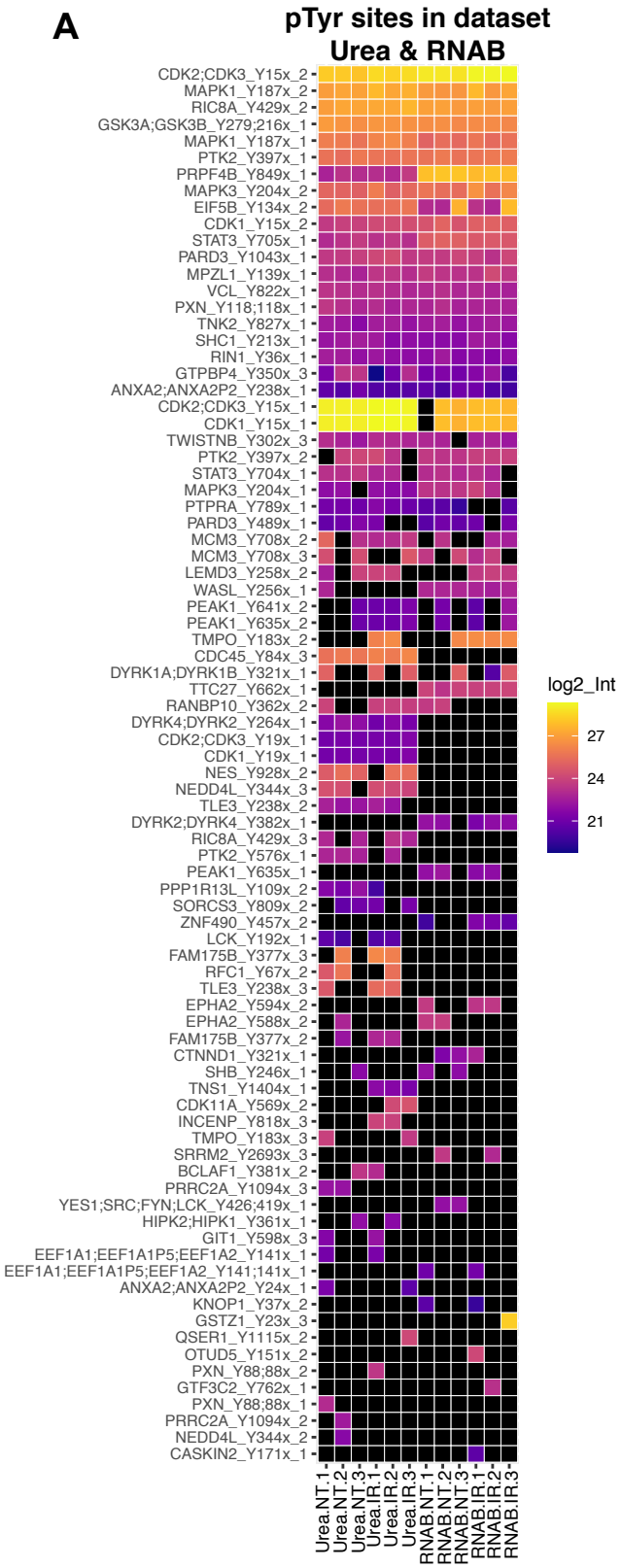

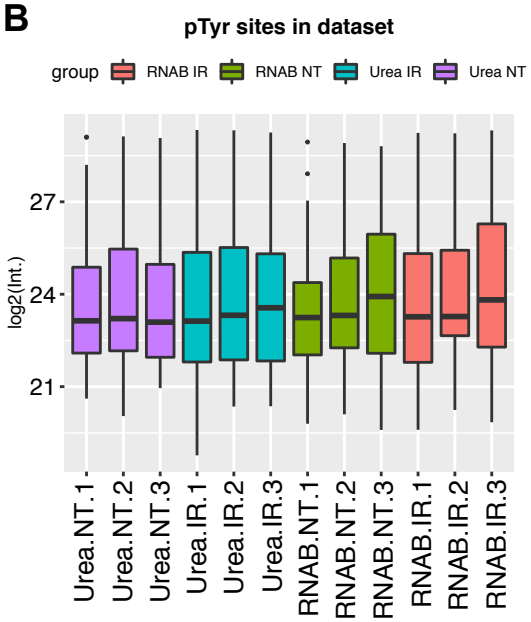

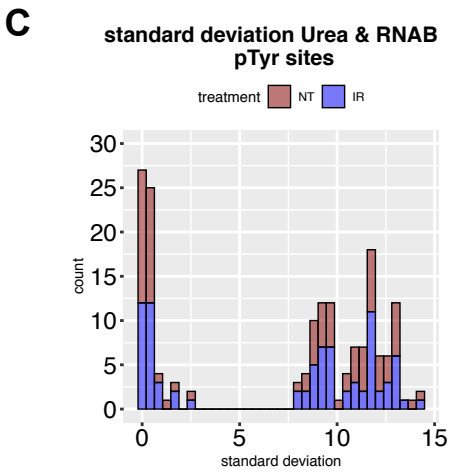

Supplementary Figure 9: U2OS cells: Comparison of pTyr sites detected in dataset.
A-C) Same as in supplementary Fig. 4. Urea and RNAB isolated samples were searched separately, i.e. with MaxQuant MBR option disabled between urea and RNAB isolated samples but enabled for samples inside the same isolation group.

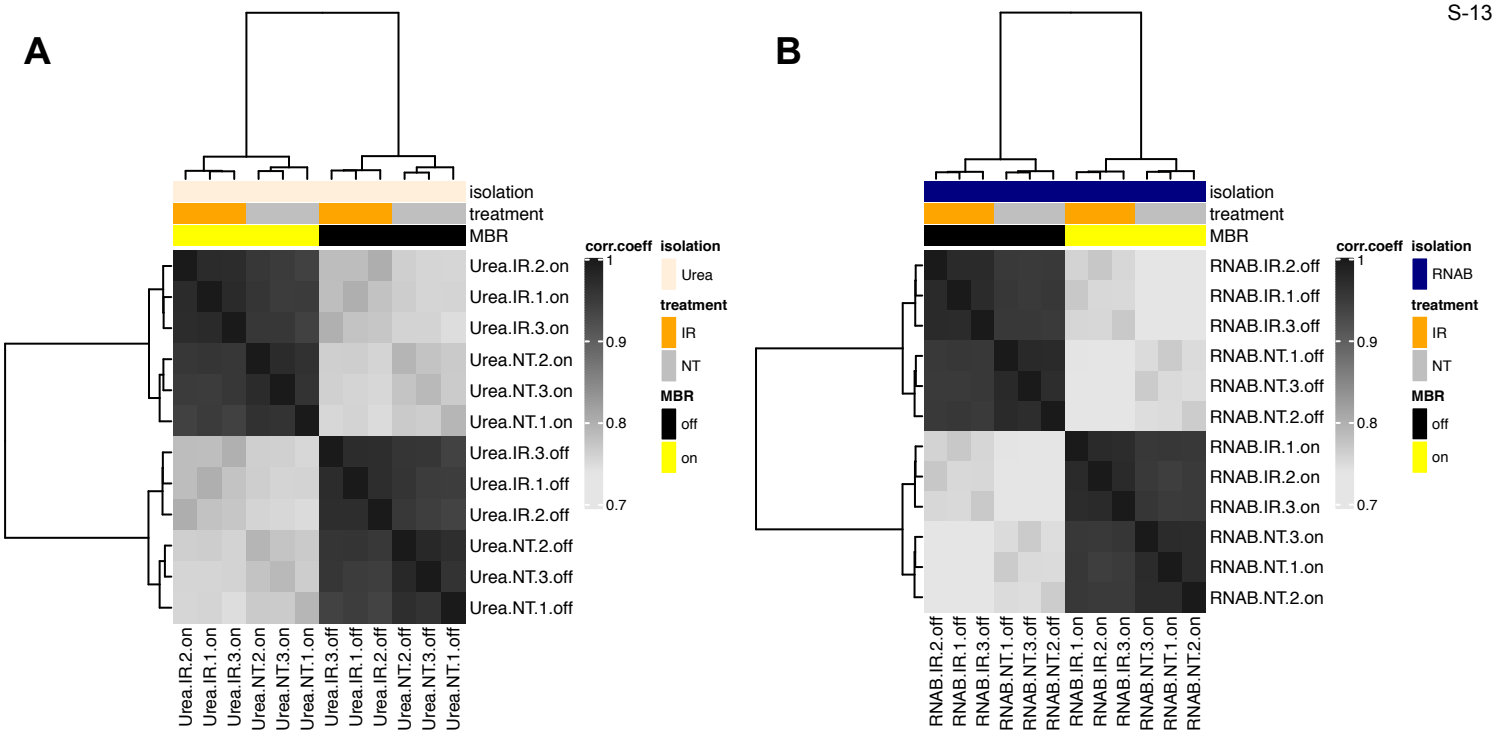

Supplementary Figure 10: U2OS cells: Correlation of urea or RNAB isolated samples with different settings for MaxQuant match betweens runs.
A) Heatmap showing the correlation between urea isolated samples with different MaxQuant match between run (MBR) options. MBR was enabled for all samples (on) or disabled (off) between urea and RNAB derived samples. Pearson correlation coefficient (corr.coeff.) is based on normalized intensity data and class 1 phosphosites. Correlation coefficient, isolation method, treatment and setting of the match between run option are color coded.
B) Same as for supplementary Fig. 10 A for RNAB samples.

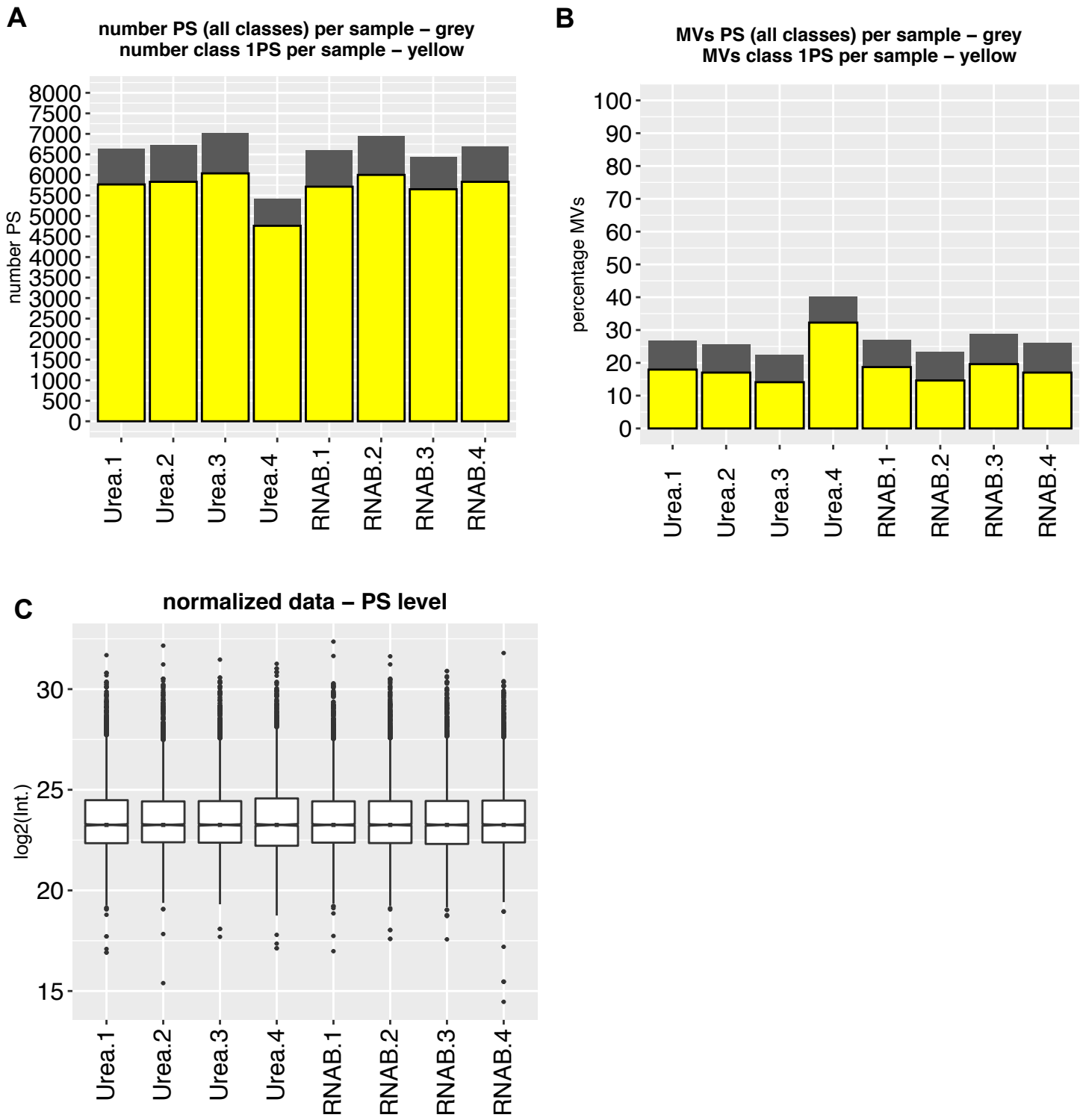

Supplementary Figure 11: Murine tissue: Phosphoproteomic profiling of mouse liver tissue after lysis with urea or RNA-Bee (RNAB).
A-C) Same as supplementary Fig. 1. MaxQuant MBR option was enabled for all samples.

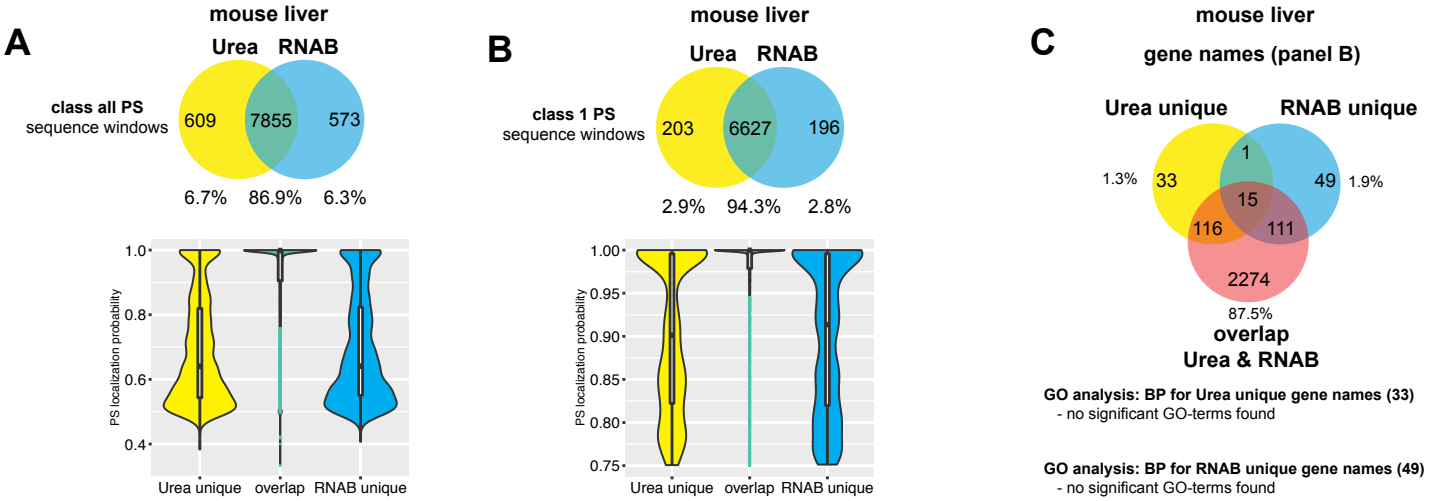

Supplementary Figure 12: Murine liver tissue: Overlap of phosphosites identified per isolation method after urea and RNA-Bee (RNAB) lysed cells.
A-C) Related to Fig. 2 A. Same as supplementary Fig. 2 A-C. MaxQuant MBR option was enabled for all samples.

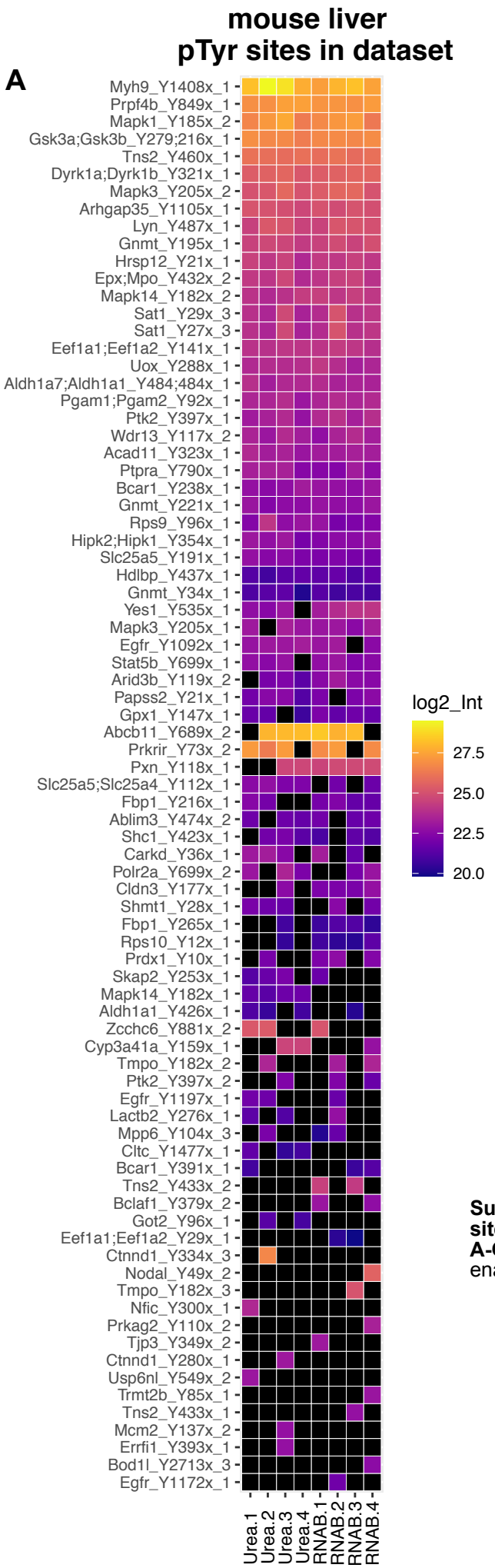

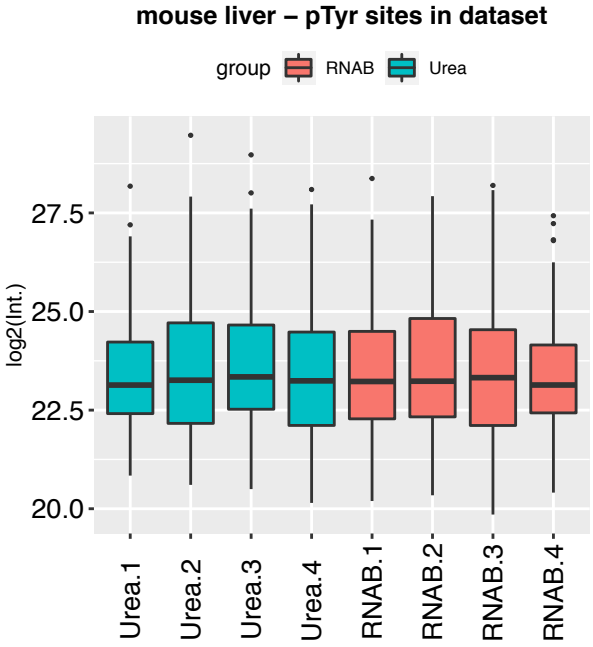

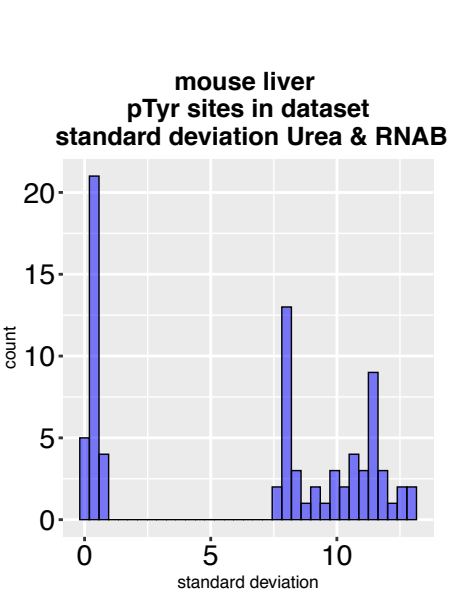

Supplementary Figure 13: Murine liver tissue: Comparison of pTyr sites detected in dataset.
A-C) Same as supplementary Fig. 4 A-C. MaxQuant MBR option was enabled for all samples.

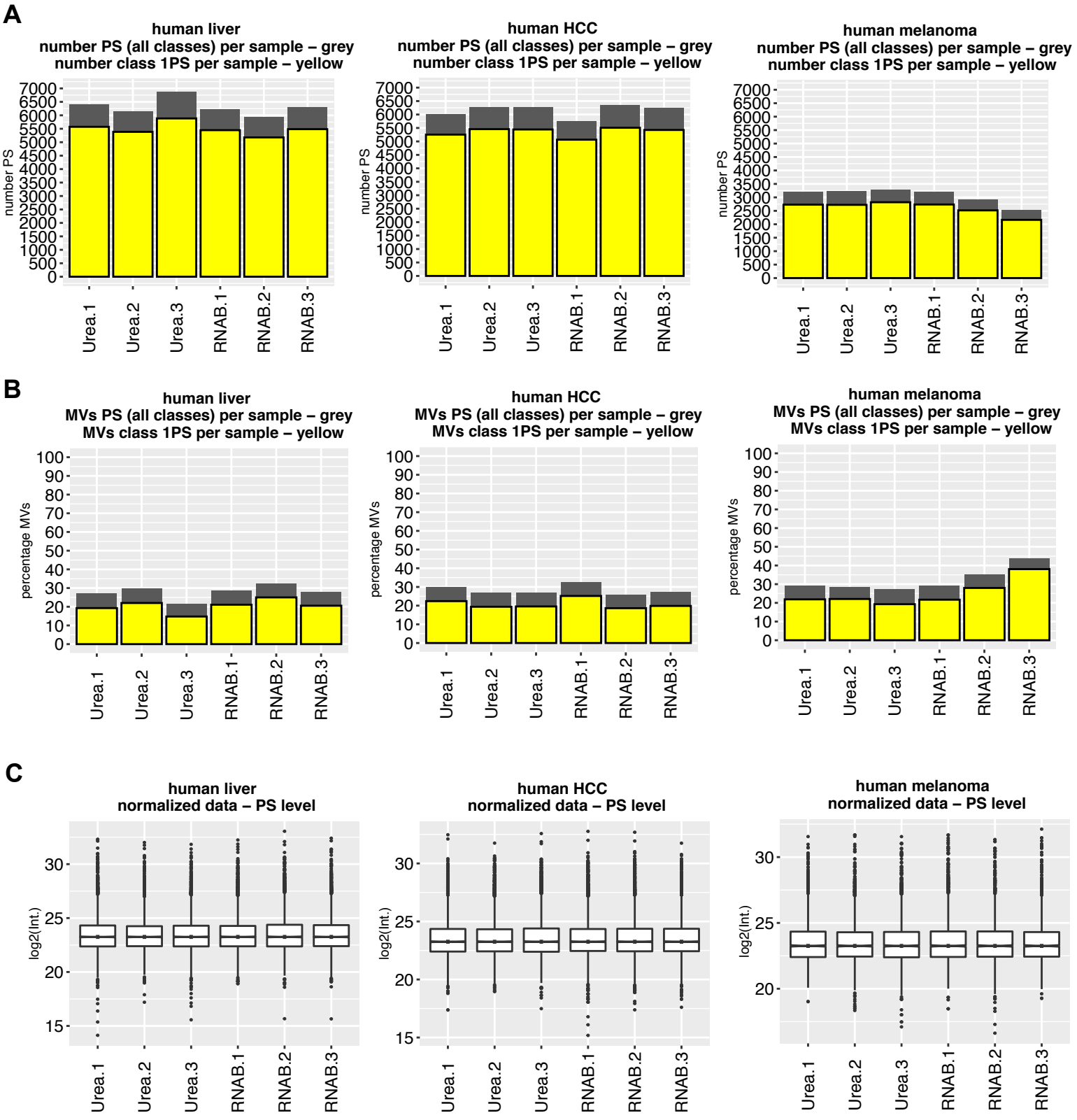

Supplementary Figure 14: Human tissue: Phosphoproteomic profiling of human liver, HCC and melanoma tissue after lysis with urea or RNA-Bee (RNAB).
A-C) Same as supplementary Fig. 1. for normal liver (left), HCC (middle) and melanoma (right). MaxQuant MBR option was enabled for all samples.

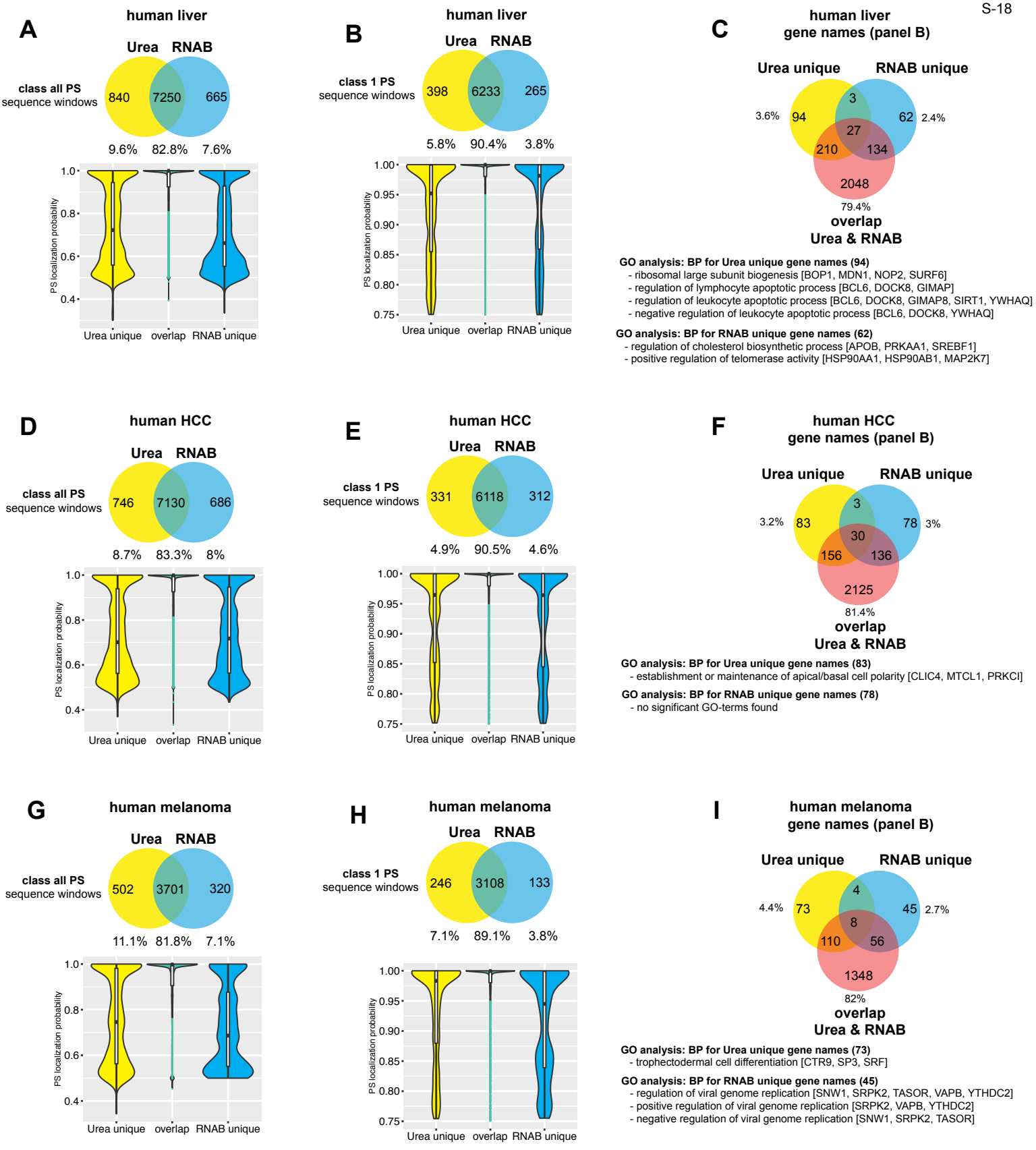

Supplementary Figure 15: Human tissue: Overlap of phosphosites identified per isolation method after urea and RNA-Bee (RNAB) lysed cells.
A-I) Related to Fig. 2 D. Same as supplementary Fig. 2 A-C for normal liver (left), HCC (middle) and melanoma (right). MaxQuant MBR option was enabled for all samples.

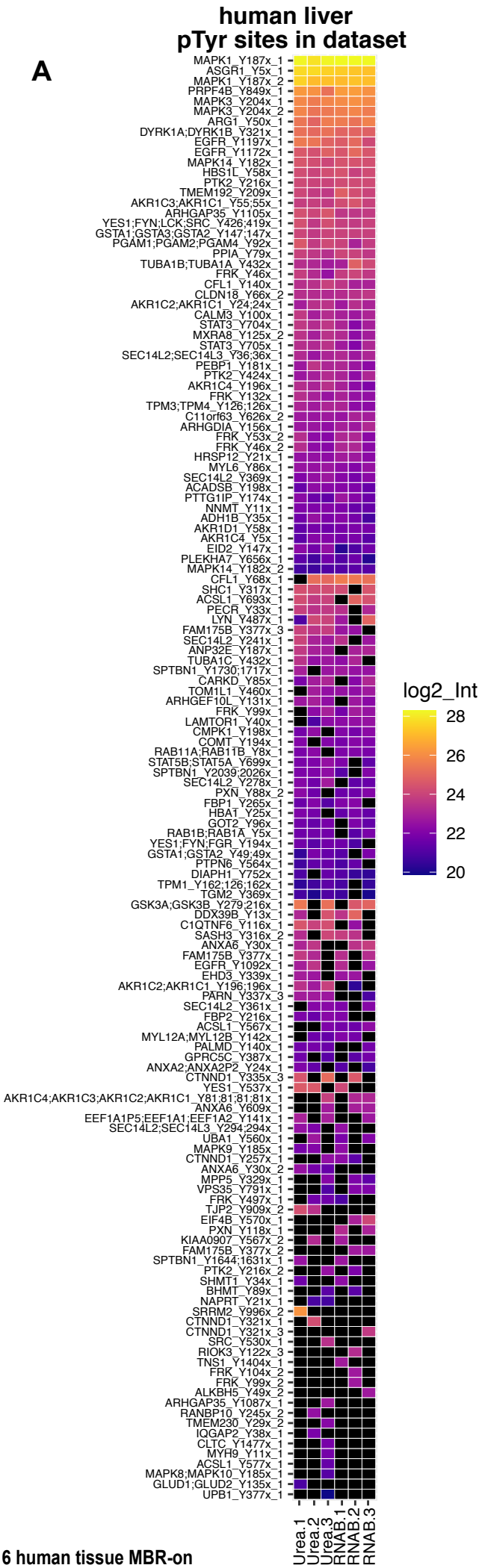

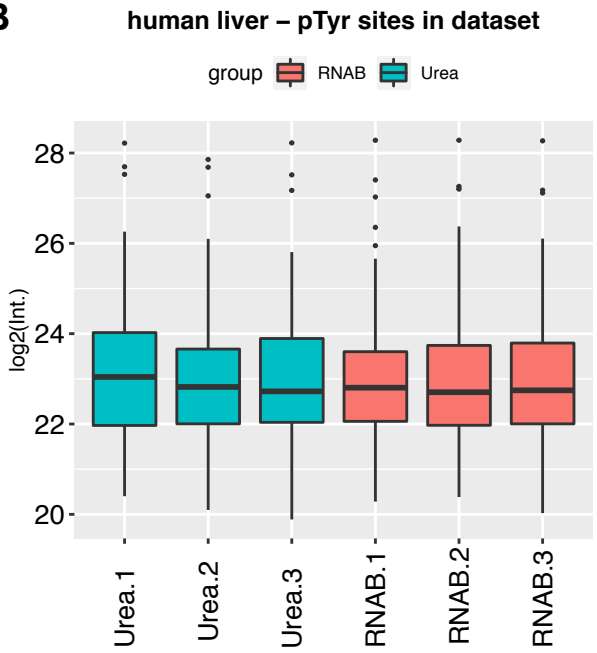

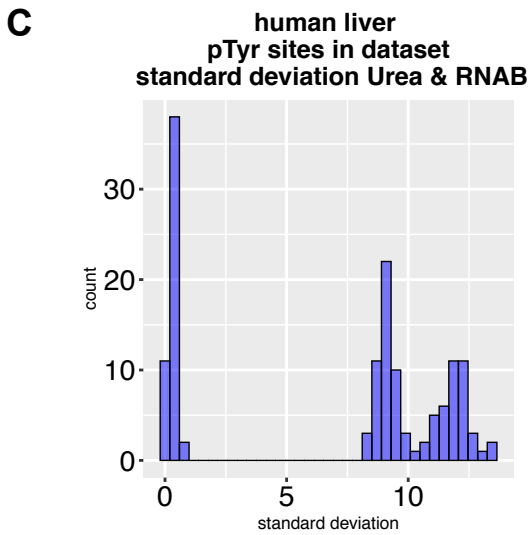

Supplementary Figure 16: Human liver tissue: Comparison of pTyr sites detected in dataset.
A-C) Same as supplementary Fig. 4 A-C. MaxQuant MBR option was enabled for all samples.

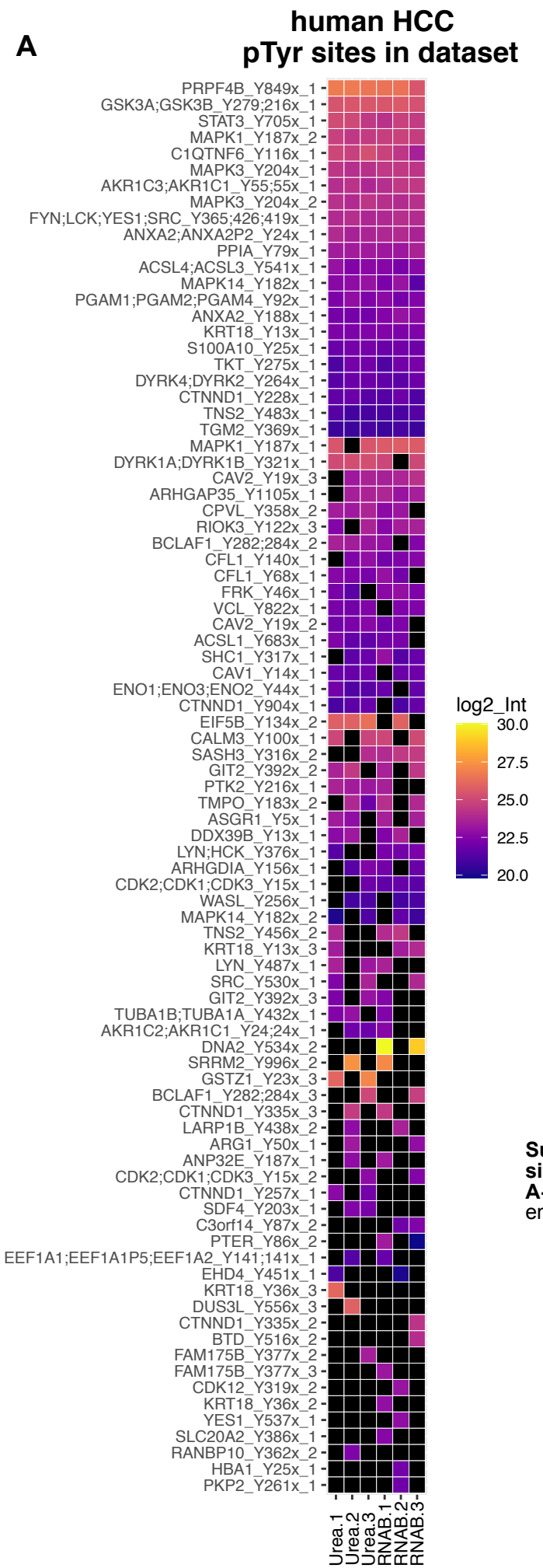

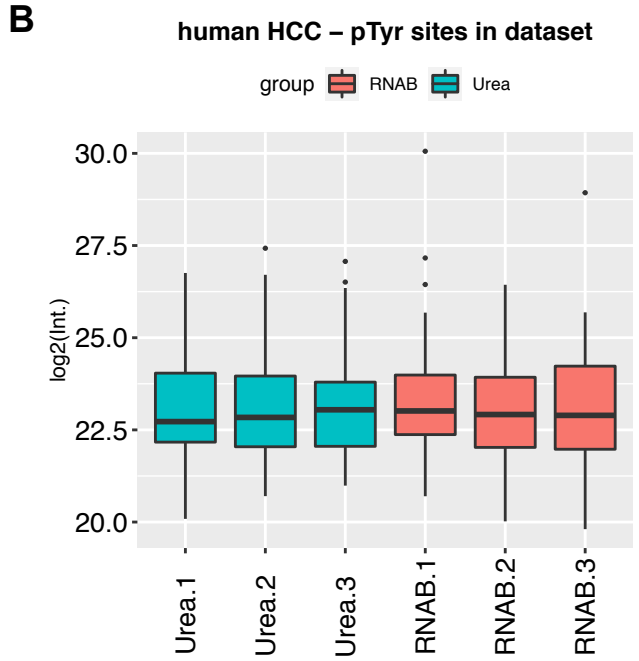

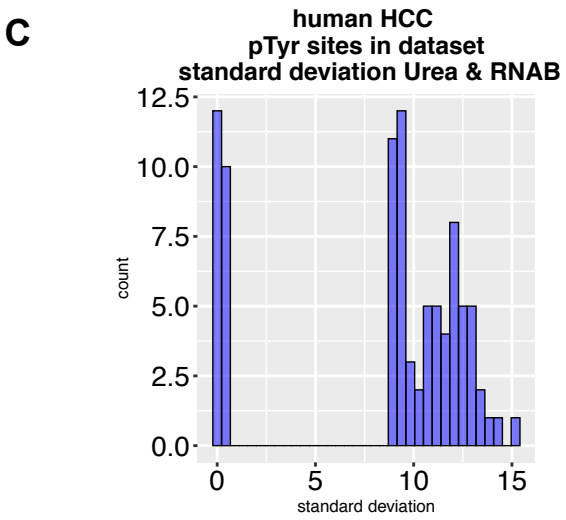

Supplementary Figure 17: Human HCC tissue: Comparison of pTyr sites detected in dataset.
A-C) Same as supplementary Fig. 4 A-C. MaxQuant MBR option was enabled for all samples.

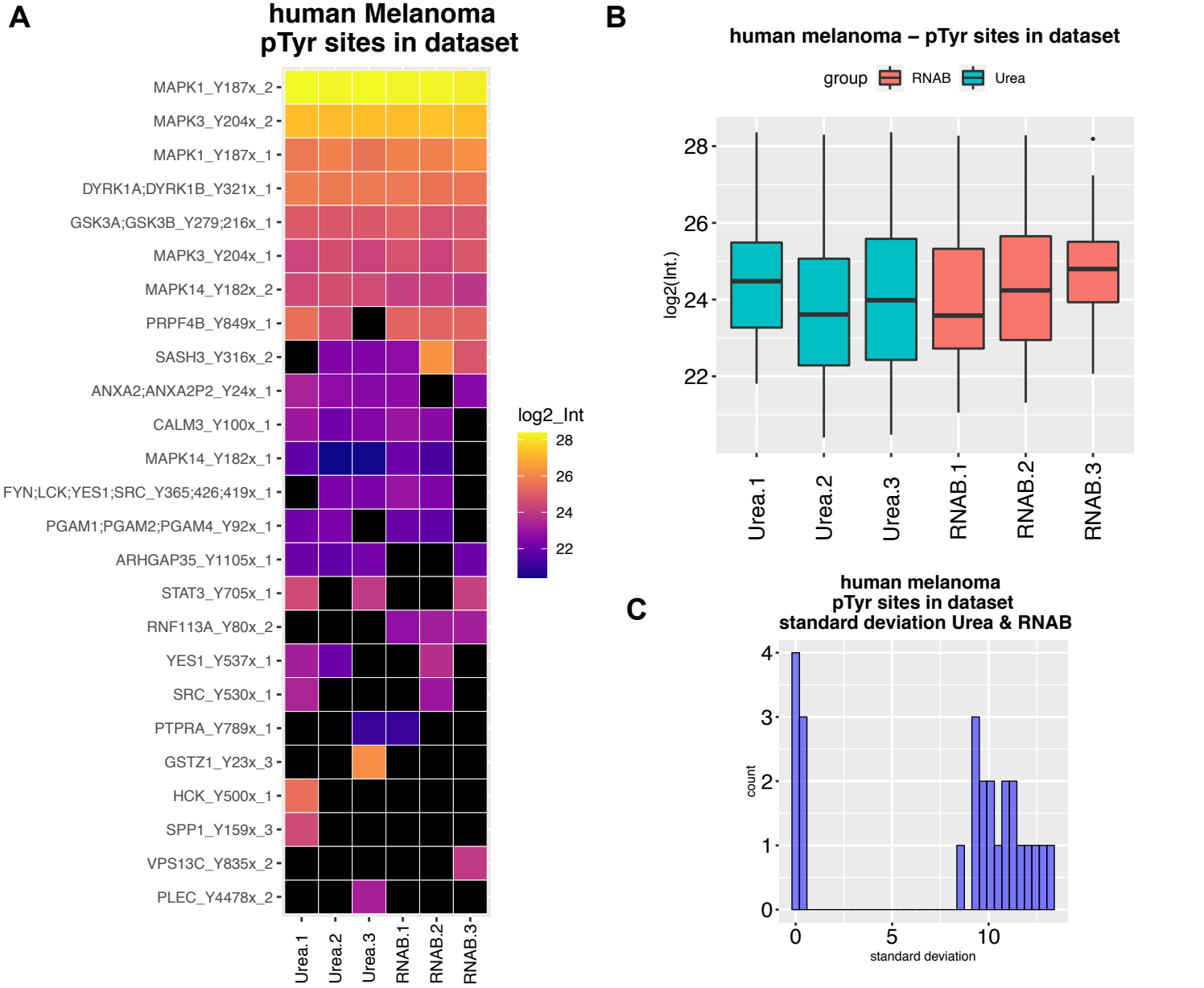

Supplementary Figure 18: Human melanoma tissue: Comparison of pTyr sites detected in dataset.
A-C) Same as supplementary Fig. 4 A-C. MaxQuant MBR option was enabled for all samples.

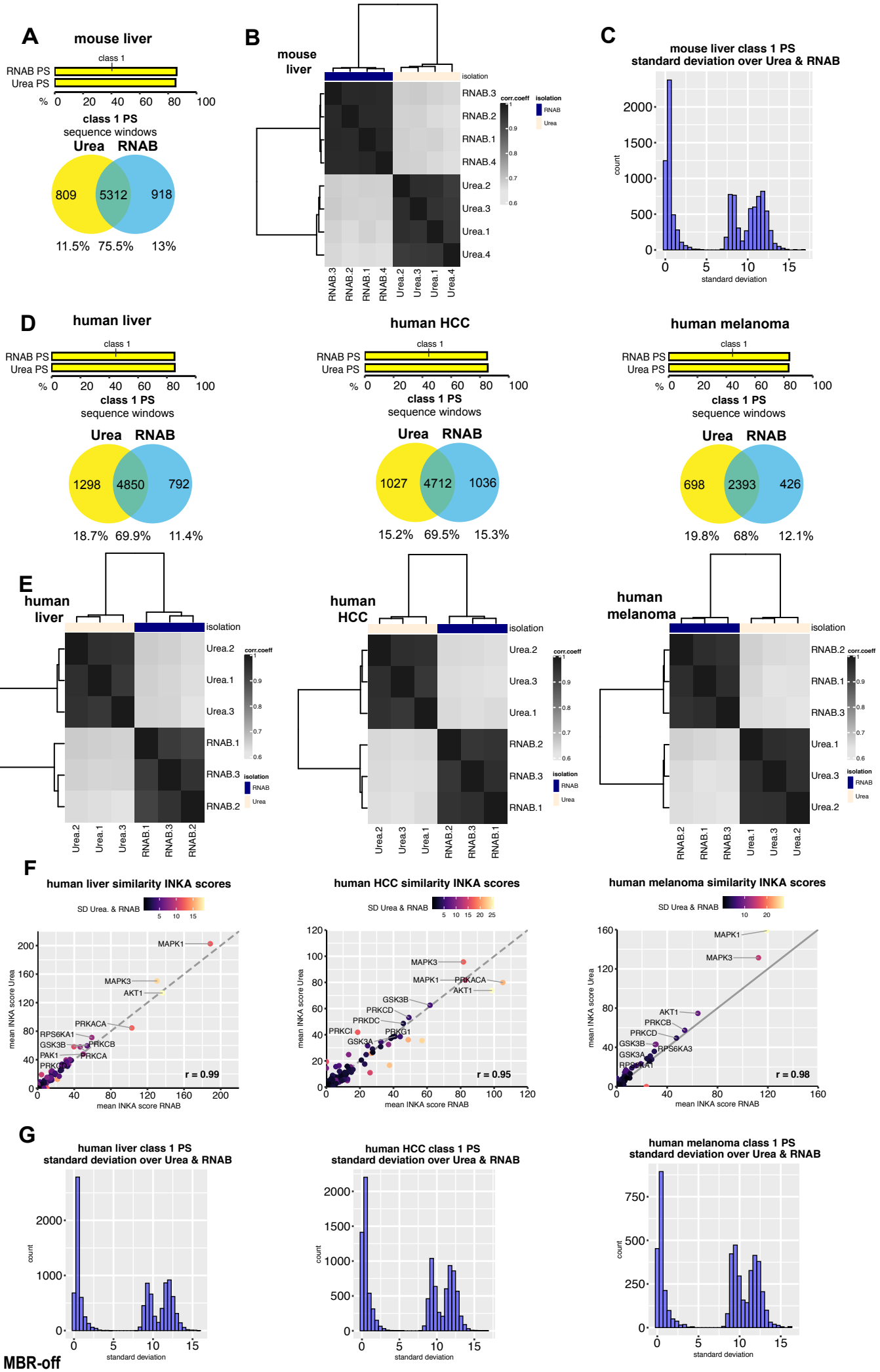

S19 tissue MBR-off

Supplementary Figure 19: Phosphoproteomic data comparison of mouse and human tissue material extracted with urea lysis buffer or RNA-Bee shows high similarity.
A-G) Same as Fig. 2. Urea and RNAB isolated samples were searched separately, i.e. with MaxQuant MBR option disabled between urea and RNAB isolated samples but enabled for samples inside the same isolation group.

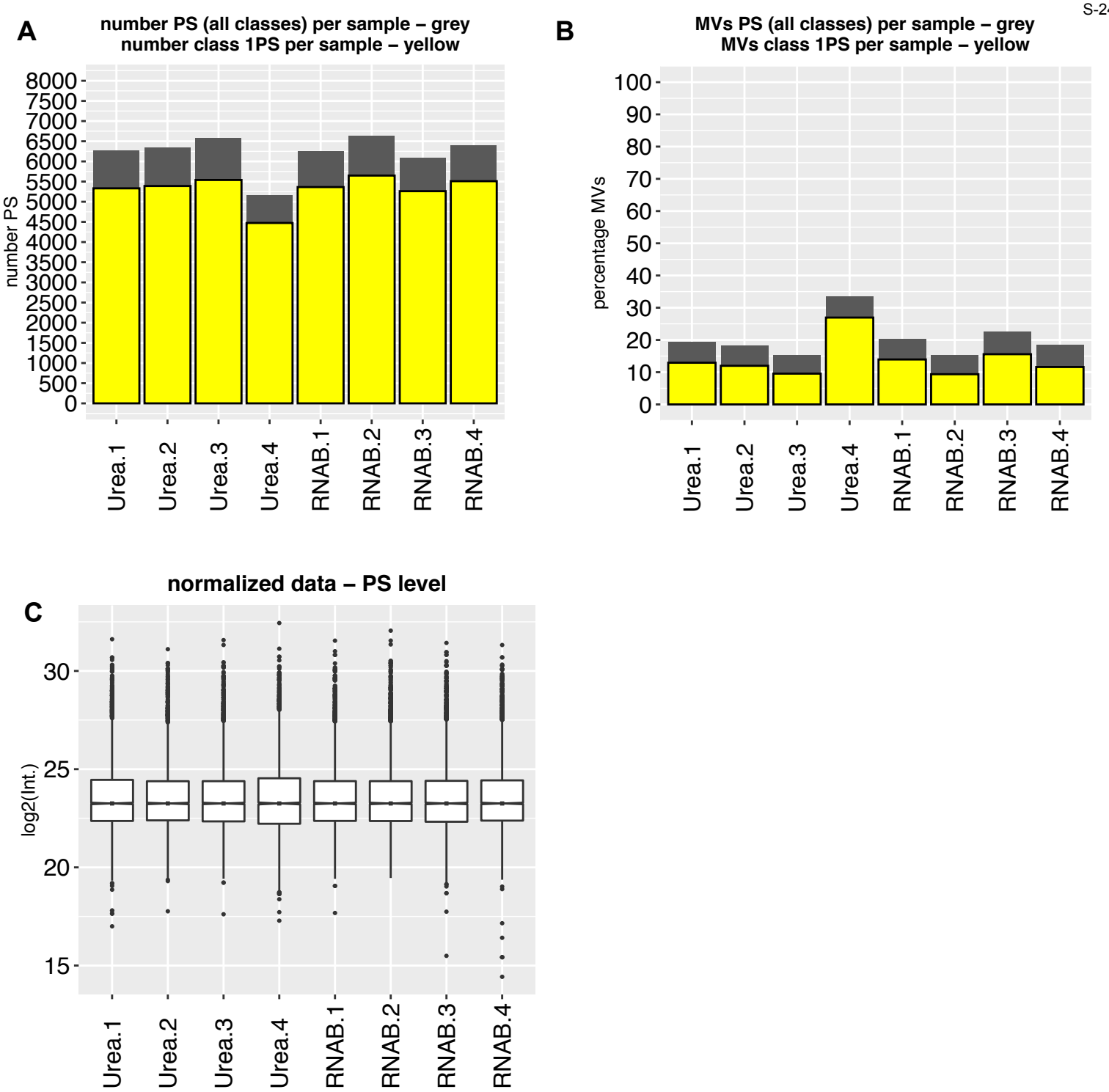

Supplementary Figure 20: Murine tissue: Phosphoproteomic profiling of mouse liver tissue after lysis with urea or RNA-Bee (RNAB).
A-C) Same as supplementary Fig. 1. Urea and RNAB isolated samples were searched separately, i.e. with MaxQuant MBR option disabled between urea and RNAB isolated samples but enabled for samples inside the same isolation group.

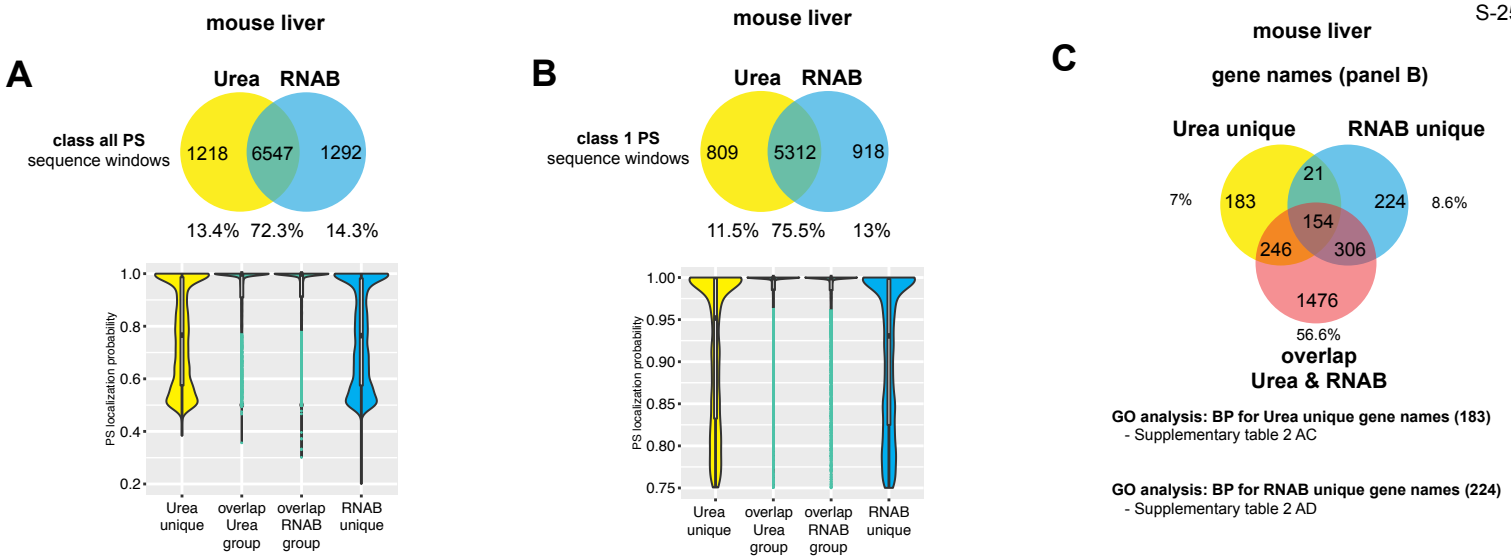

GO analysis: BP for Urea unique gene names (183)
- Supplementary table 2 AC

GO analysis: BP for RNAB unique gene names (224)
- Supplementary table 2 AD

Supplementary Figure 21: Murine liver tissue: Overlap of phosphosites identified per isolation method after urea and RNA-Bee (RNAB) lysed cells.
A-C) Related to Fig. 2 A. Same as supplementary Fig. 2 A-C. Urea and RNAB isolated samples were searched separately, i.e. with MaxQuant MBR option disabled between urea and RNAB isolated samples but enabled for samples inside the same isolation group.

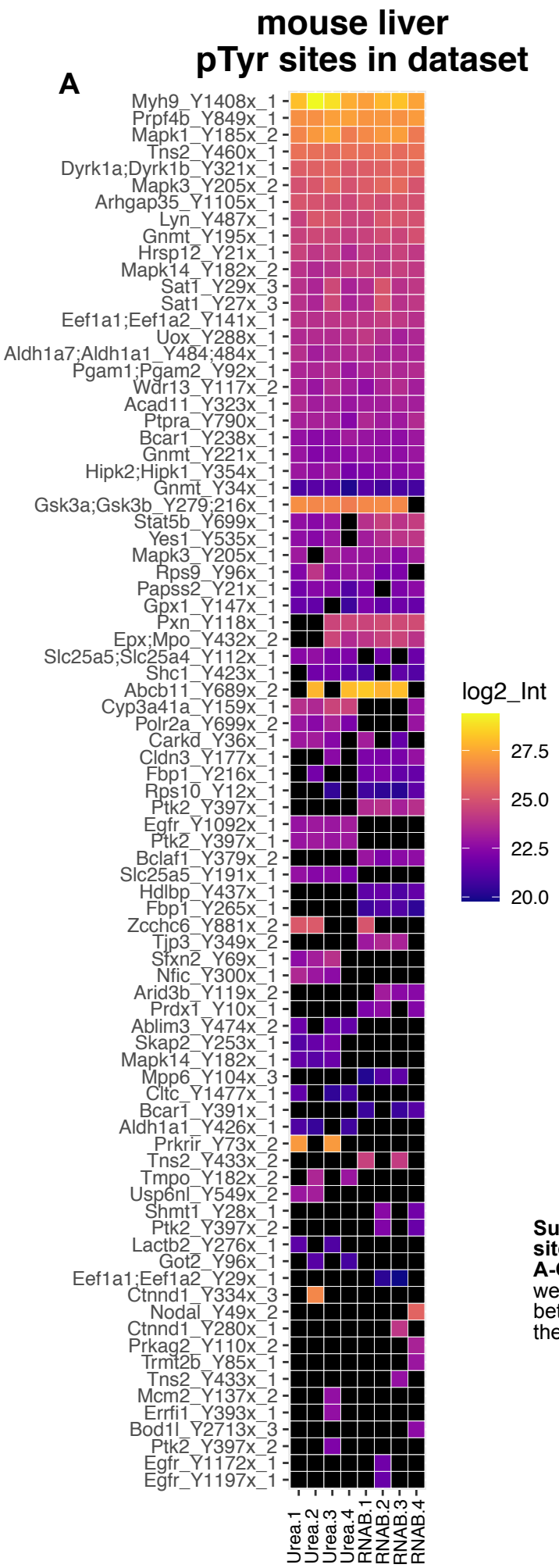

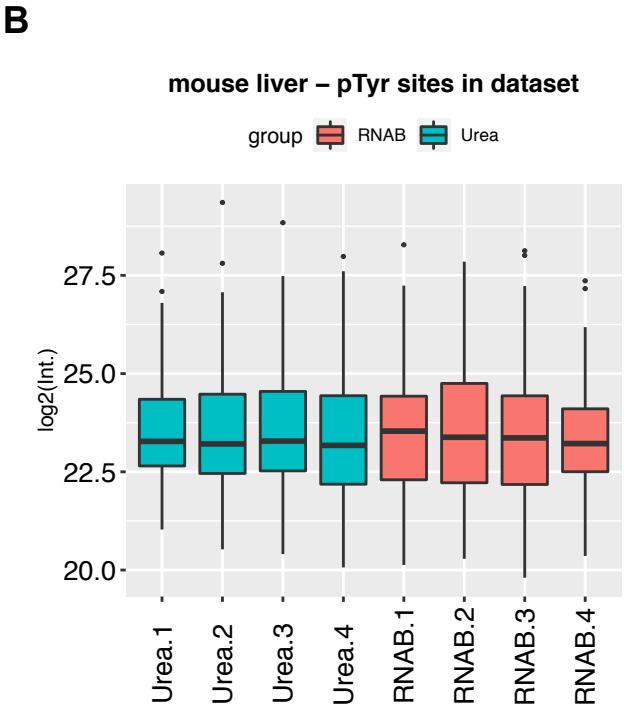

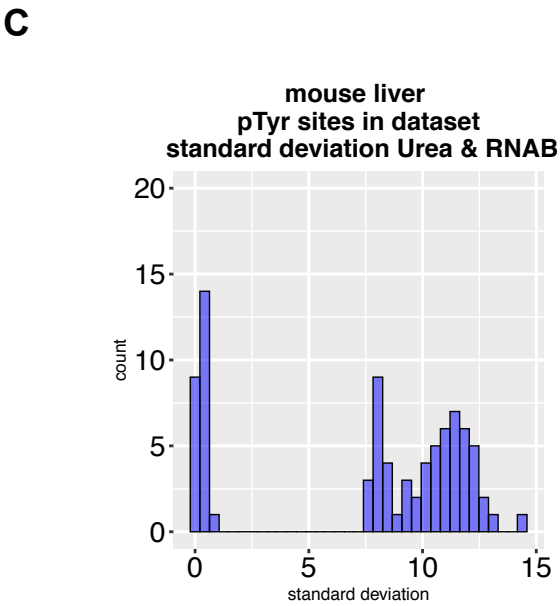

Supplementary Figure 22: Murine liver tissue: Comparison of pTyr sites detected in dataset.
A-C) Same as supplementary Fig. 4 A-C. Urea and RNAB isolated samples were searched separately, i.e. with MaxQuant MBR option disabled between urea and RNAB isolated samples but enabled for samples inside the same isolation group.

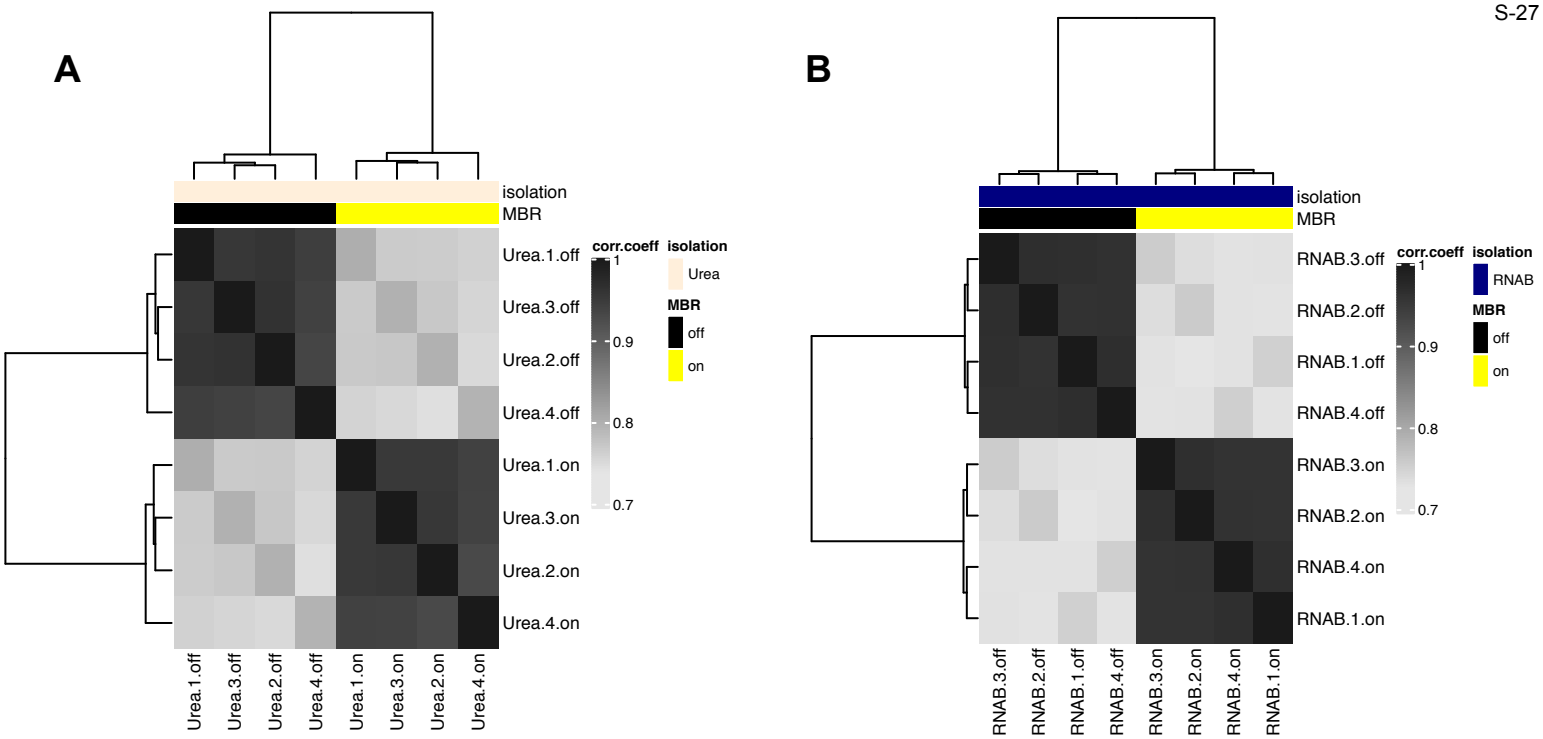

Supplementary Figure 23: Murine liver tissue: Correlation of urea or RNAB isolated samples with different settings for MaxQuant match betweens runs.
A) Heatmap showing the correlation between urea isolated samples with different MaxQuant match between run (MBR) options. MBR was enabled for all samples (on) or disabled (off) between urea and RNAB derived samples. Pearson correlation coefficient (corr.coeff.) is based on normalized intensity data and class 1 phosphosites. Correlation coefficient, isolation method, treatment and setting of the match between run option are color coded.
B) Same as for supplementary Fig. 23 A for RNAB samples.

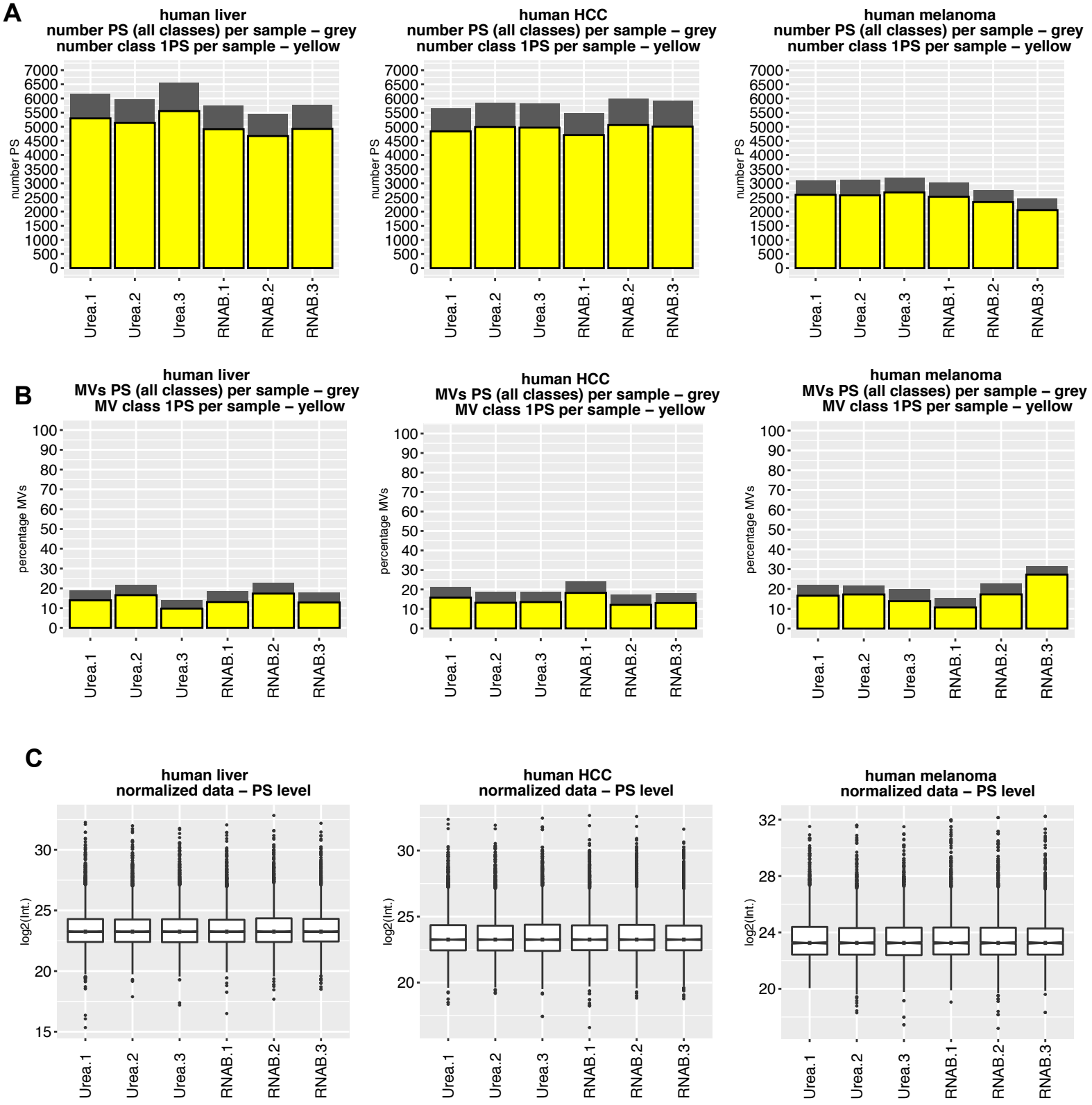

Supplementary Figure 24: Human tissue: Phosphoproteomic profiling of human liver, HCC and melanoma tissue after lysis with urea or RNA-Bee (RNAB).
A-C) Same as supplementary Fig. 1. for normal liver (left), HCC (middle) and melanoma (right). Urea and RNAB isolated samples were searched separately, i.e. with MaxQuant MBR option disabled between urea and RNAB isolated samples but enabled for samples inside the same isolation group.

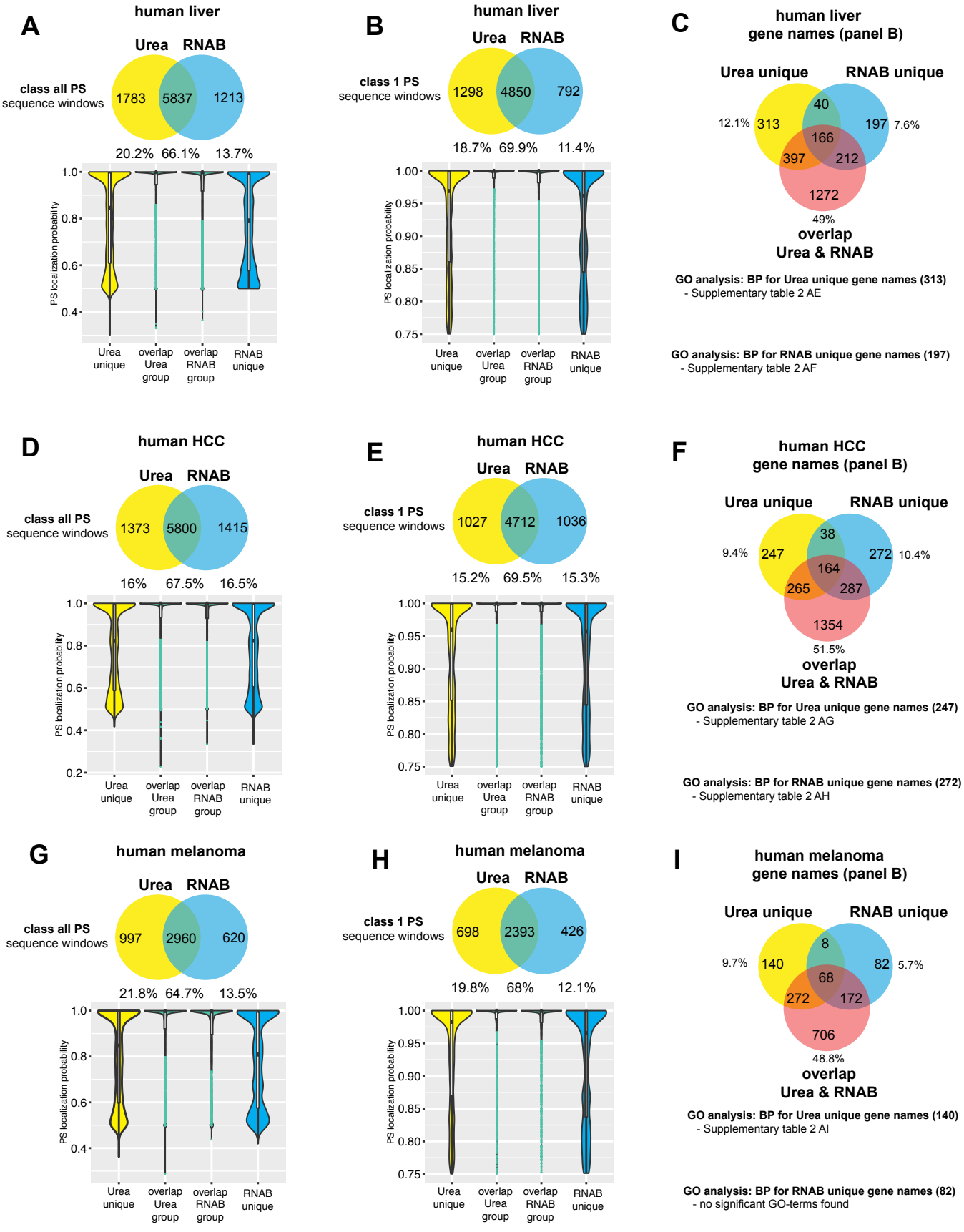

Supplementary Figure 25: Human tissue: Overlap of phosphosites identified per isolation method after urea and RNA-Bee (RNAB) lysed cells.
A-I) Related to Fig. 2 D. Same as supplementary Fig. 2 A-C for normal liver (left), HCC (middle) and melanoma (right). Urea and RNAB isolated samples were searched separately, i.e. with MaxQuant MBR option disabled between urea and RNAB isolated samples but enabled for samples inside the same isolation group.

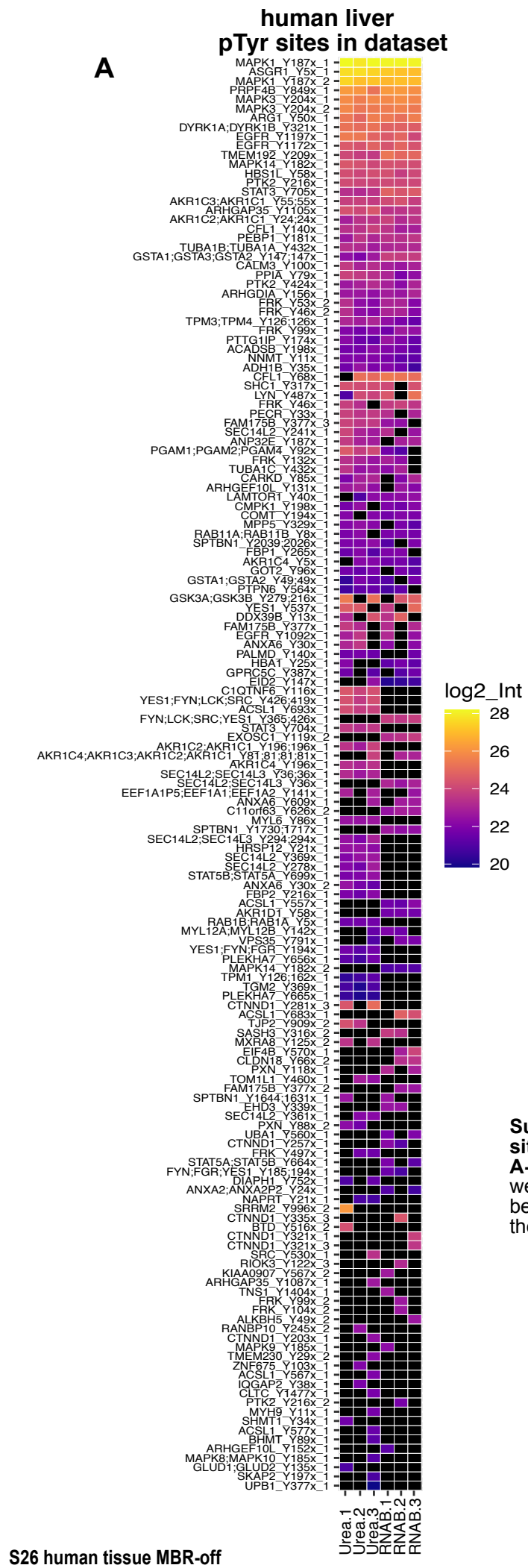

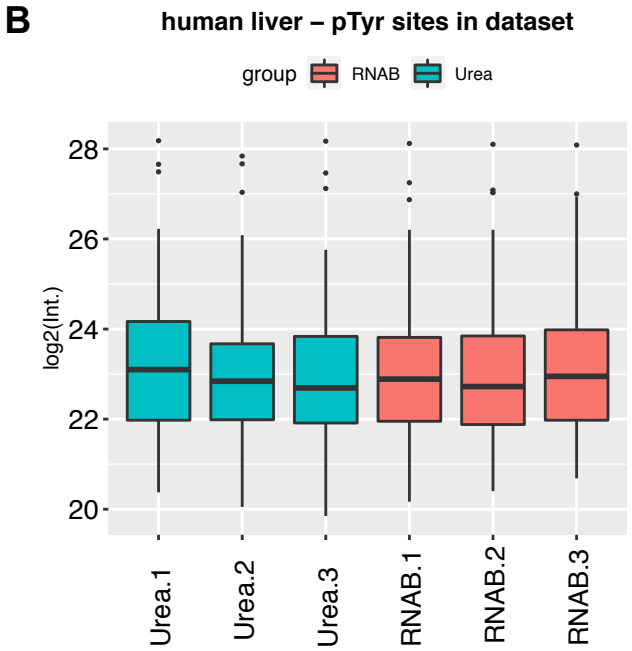

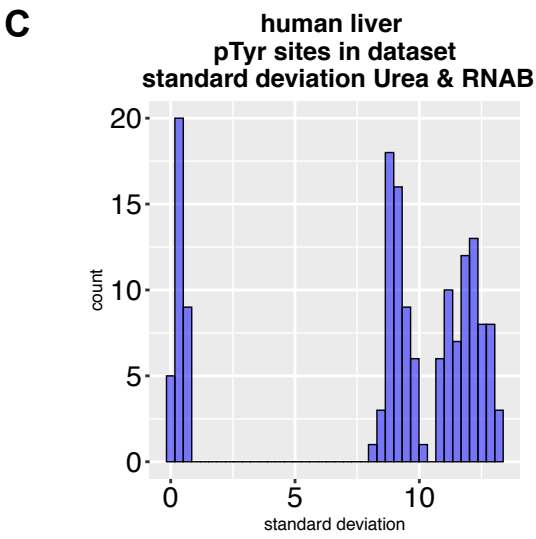

Supplementary Figure 26: Human liver tissue: Comparison of pTyr sites detected in dataset.
A-C) Same as supplementary Fig. 4 A-C. Urea and RNAB isolated samples were searched separately, i.e. with MaxQuant MBR option disabled between urea and RNAB isolated samples but enabled for samples inside the same isolation group.

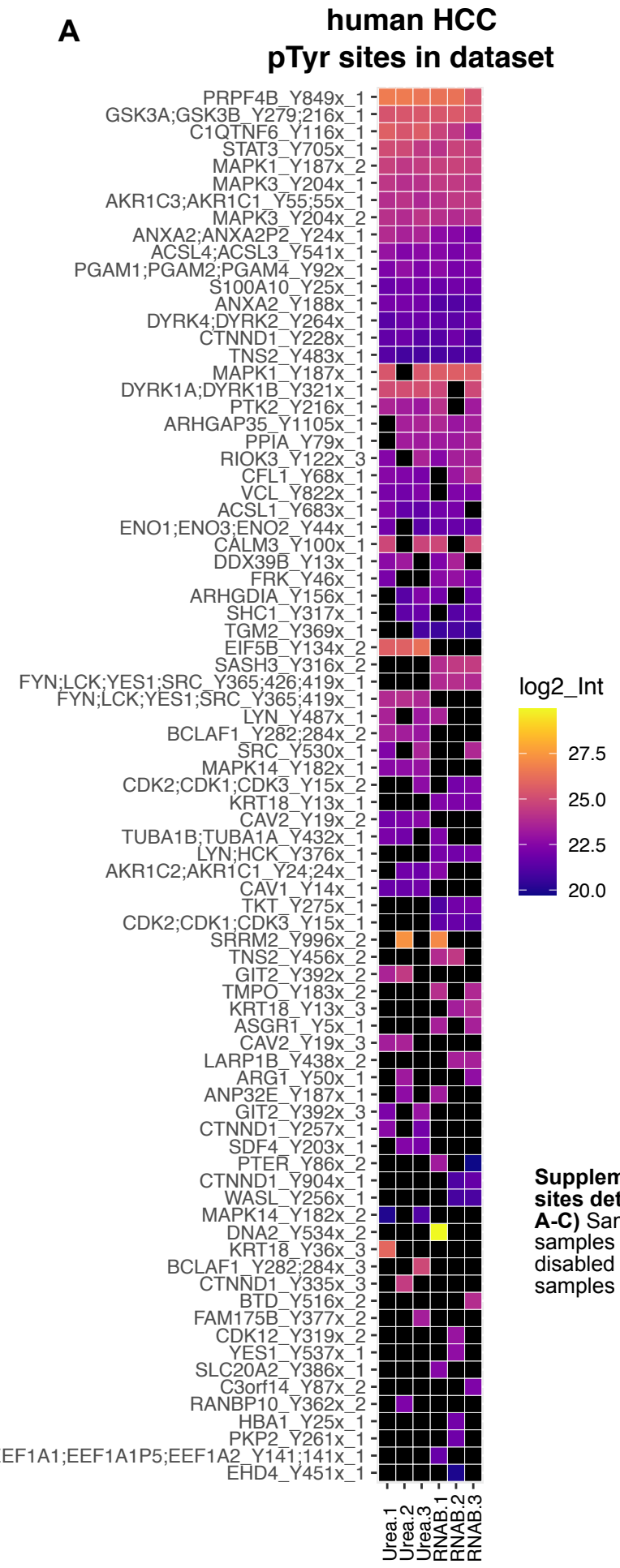

Supplementary Figure 27: Human HCC tissue: Comparison of pTyr sites detected in dataset.
A-C) Same as supplementary Fig. 4 A-C. Urea and RNAB isolated samples were searched separately, i.e. with MaxQuant MBR option disabled between urea and RNAB isolated samples but enabled for samples inside the same isolation group.

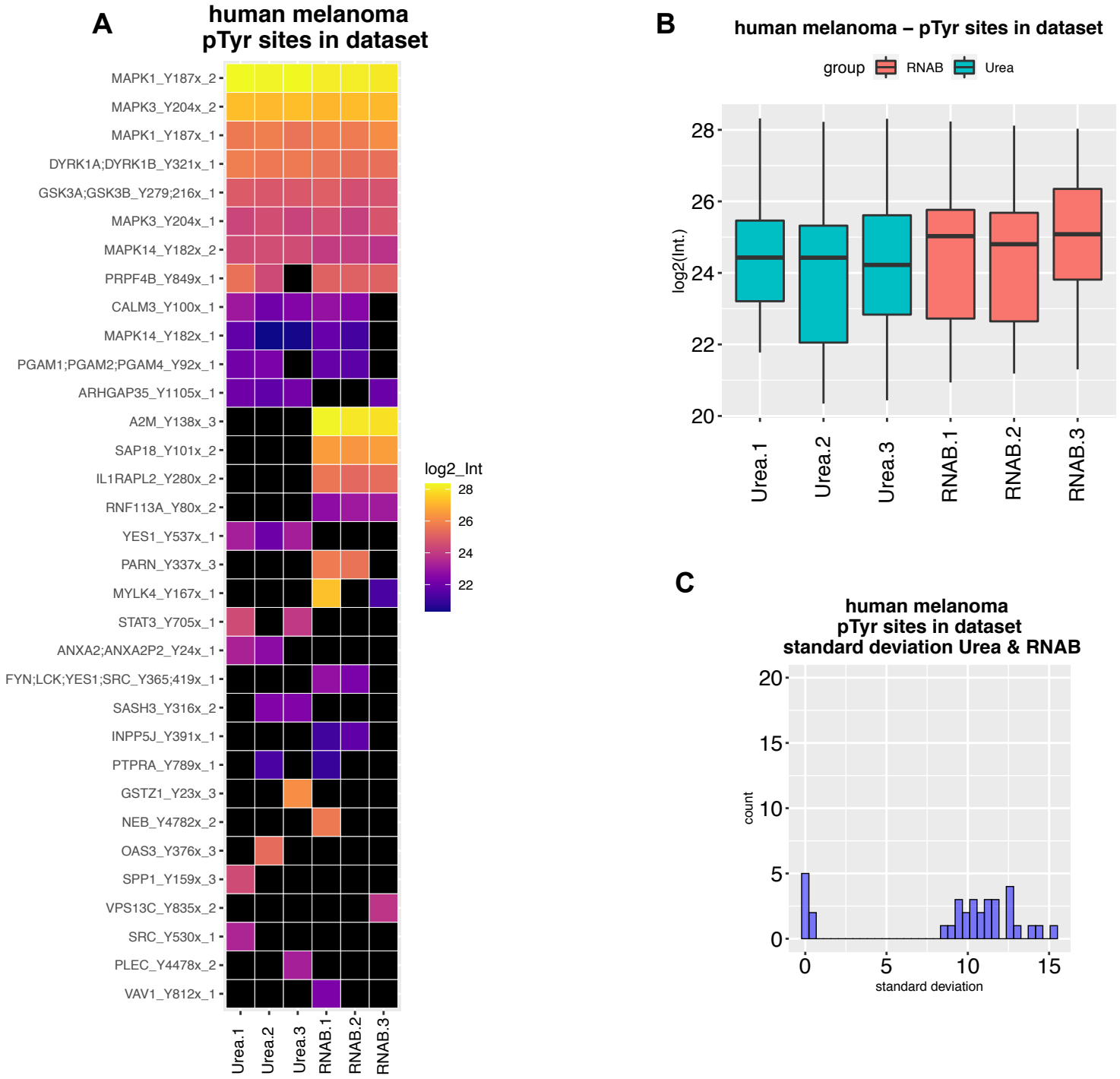

Supplementary Figure 28: Human melanoma tissue: Comparison of pTyr sites detected in dataset.
A-C) Same as supplementary Fig. 4 A-C. Urea and RNAB isolated samples were searched separately, i.e. with MaxQuant MBR option disabled between urea and RNAB isolated samples but enabled for samples inside the same isolation group.

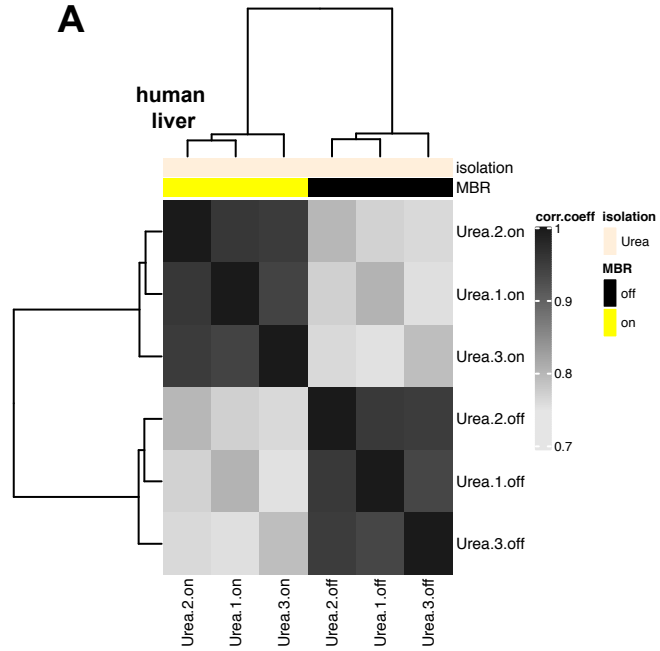
A
human liver
isolation
MBR
Urea.2.on
Urea.1.on
Urea.3.on
Urea.2.off
Urea.1.off
Urea.3.off
corr.coeff
1
0.9
0.8
0.7
isolation
Urea
MBR
off
on

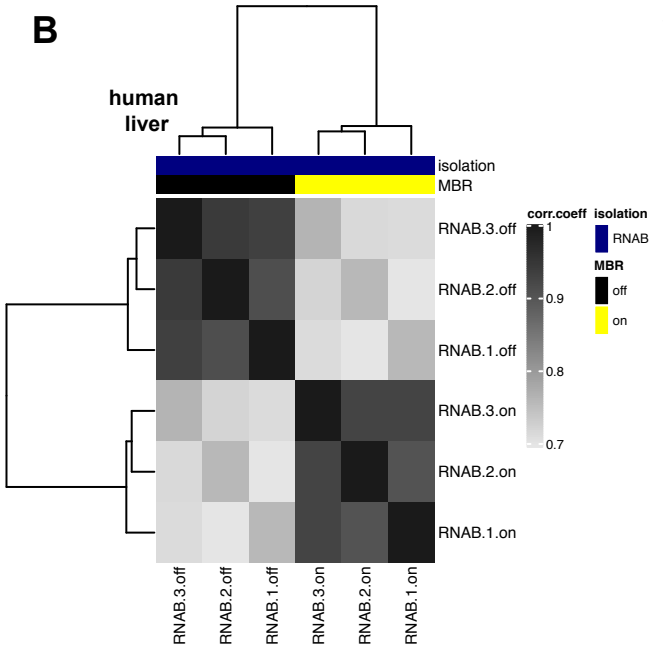
B
human liver
isolation
MBR
RNAB.3.off
RNAB.2.off
RNAB.1.off
RNAB.3.on
RNAB.2.on
RNAB.1.on
corr.coeff
1
0.9
0.8
0.7
isolation
RNAB
MBR
off
on

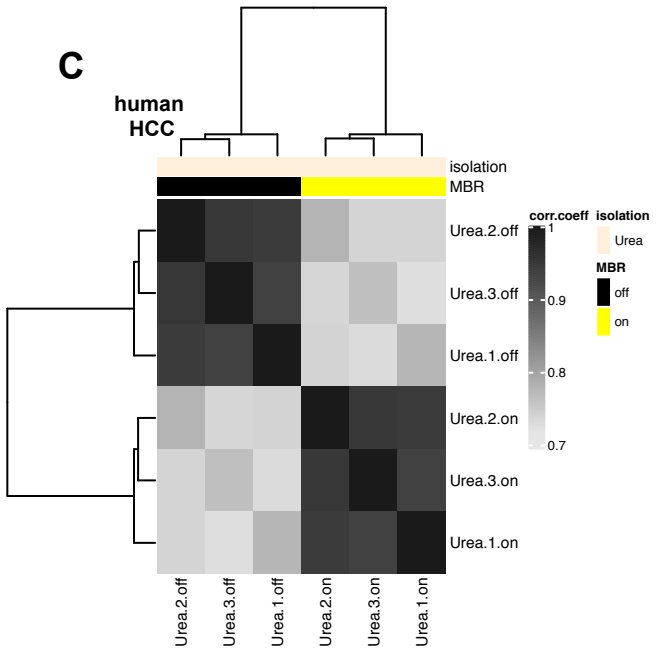
C
human HCC
isolation
MBR
Urea.2.off
Urea.3.off
Urea.1.off
Urea.2.on
Urea.3.on
Urea.1.on
corr.coeff
1
0.9
0.8
0.7
isolation
Urea
MBR
off
on

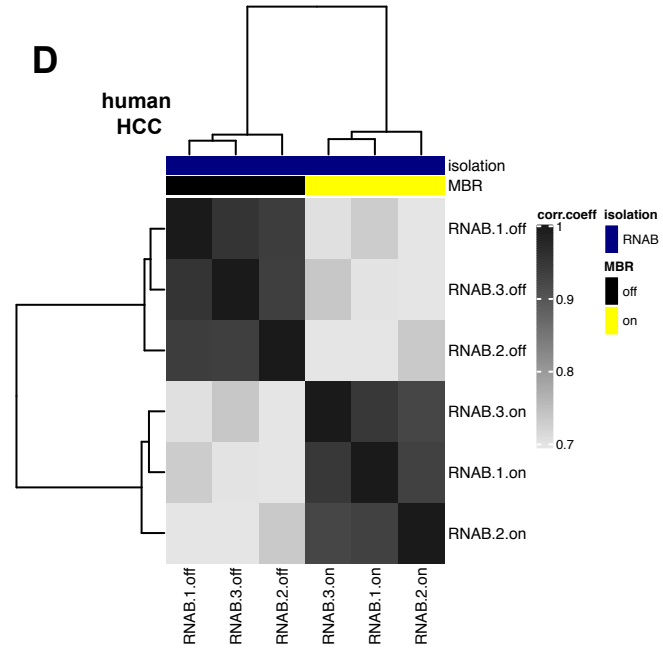
D
human HCC
isolation
MBR
RNAB.1.off
RNAB.3.off
RNAB.2.off
RNAB.3.on
RNAB.1.on
RNAB.2.on
corr.coeff
1
0.9
0.8
0.7
isolation
RNAB
MBR
off
on

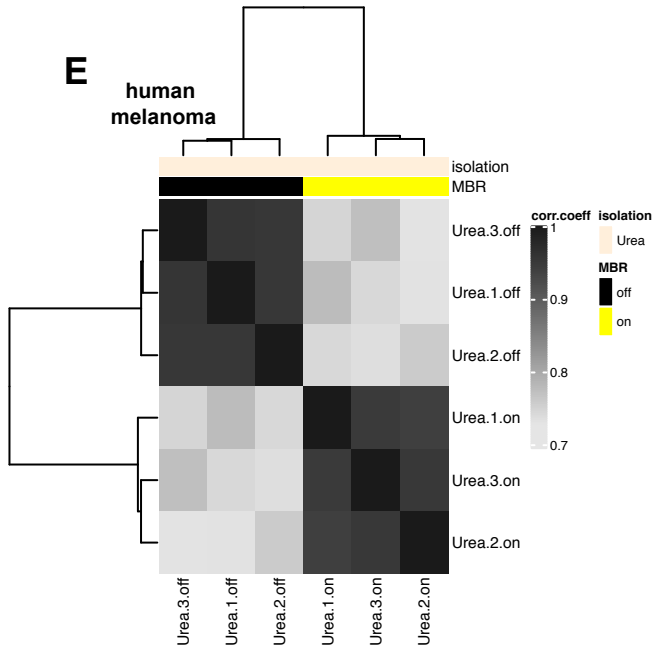
E
human melanoma
isolation
MBR
Urea.3.off
Urea.1.off
Urea.2.off
Urea.1.on
Urea.3.on
Urea.2.on
corr.coeff
1
0.9
0.8
0.7
isolation
Urea
MBR
off
on

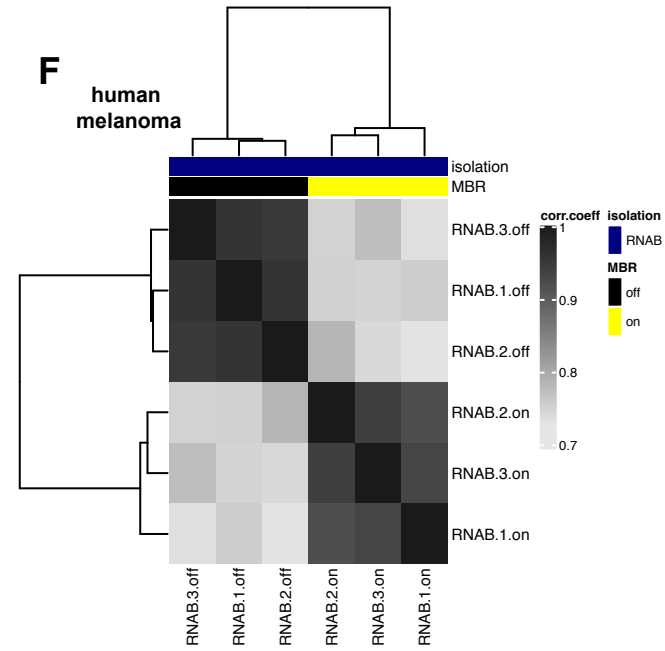
F
human melanoma
isolation
MBR
RNAB.3.off
RNAB.1.off
RNAB.2.off
RNAB.2.on
RNAB.3.on
RNAB.1.on
corr.coeff
1
0.9
0.8
0.7
isolation
RNAB
MBR
off
on

Supplementary Figure 29: Human tissue: Correlation of urea or RNAB isolated samples with different settings for MaxQuant match betweens runs.
A) Heatmap showing the correlation between urea isolated samples for human liver with different MaxQuant match between run (MBR) options. MBR was enabled for all samples (on) or disabled (off) between urea and RNAB derived samples. Pearson correlation coefficient (corr.coeff.) is based on normalized intensity data and class 1 phosphosites. Correlation coefficient, isolation method, treatment and setting of the match between run option are color coded.
B) Same as for supplementary Fig. 29 A for human liver RNAB samples.
C) Same as for supplementary Fig. 29 A for human HCC urea samples.
D) Same as for supplementary Fig. 29 A for human HCC RNAB samples.
E) Same as for supplementary Fig. 29 A for human melanoma urea samples.
F) Same as for supplementary Fig. 29 A for human melanoma RNAB samples.

Legend supplementary Table 1 (separate Excel file). MaxQuant match between runs option was enabled for all samples (MBR-on).

- Sample overview.
- Raw file overview.

A) Shortened MaxQuant output after exclusion of reverse hits, contaminants and zero-sum rows. Basis for determination of phosphosite numbers and missing values. **U2OS cells.**
B) Samplewise determined number of all class phosphosites, missing values and their percentages. Based on A. **U2OS cells.**
C) Samplewise determined number of class 1 phosphosites, missing values and their percentages. Based on A. **U2OS cells.**
D) Converted data matrix A, reshaped to account for the multiplicity of phosphorylations. Data were log2 transformed and normalized. **U2OS cells.**
E) Scores from inferred kinase activity (INKA) analysis. **U2OS cells.**
F) Phosphosite specific signature analysis (PTM-SEA) result for comparison of untreated and irradiated urea lysed U2OS cells.
G) Phosphosite specific signature analysis (PTM-SEA) result for comparison of untreated and irradiated RNAB lysed U2OS cells.
H) Shortend MaxQuant output after exclusion of reverse hits, contaminants and zero-sum rows. Basis for determination of phosphosite numbers and missing values. **Mouse liver.**
I) Samplewise determined number of all class phosphosites, missing values and their percentages. Based on H. **Mouse liver.**
J) Samplewise determined number of class 1 phosphosites, missing values and their percentages. Based on H. **Mouse liver.**
K) Converted data matrix H, expanded to account for the multiplicity of phosphorylations. Data were log2 transformed and normalized. **Mouse liver.**
L) Shortend MaxQuant output after exclusion of reverse hits, contaminants and zero-sum rows. Basis for determination of phosphosite numbers and missing values. **Human liver.**
M) Samplewise determined number of all class phosphosites, missing values and their percentages. Based on L. **Human liver.**
N) Samplewise determined number of class 1 phosphosites, missing values and their percentages. Based on L. **Human liver.**
O) Converted data matrix L, expanded to account for the multiplicity of phosphorylations. Data were log2 transformed and normalized. **Human liver.**
P) Scores from inferred kinase activity (INKA) analysis. **Human liver.**
Q) Shortend MaxQuant output after exclusion of reverse hits, contaminants and zero-sum rows. Basis for determination of phosphosite numbers and missing values. **Human HCC.**
R) Samplewise determined number of all class phosphosites, missing values and their percentages. Based on Q. **Human HCC.**
S) Samplewise determined number of class 1 phosphosites, missing values and their percentages. Based on Q. **Human HCC.**
T) Converted data matrix Q, expanded to account for the multiplicity of phosphorylations. Data were log2 transformed and normalized. **Human HCC.**
U) Scores from inferred kinase activity (INKA) analysis. **Human HCC.**
V) Shortend MaxQuant output after exclusion of reverse hits, contaminants and zero-sum rows. Basis for determination of phosphosite numbers and missing values. **Human melanoma.**
W) Samplewise determined number of all class phosphosites, missing values and their percentages. Based on V. **Human melanoma.**
X) Samplewise determined number of class 1 phosphosites, missing values and their percentages. Based on V. **Human melanoma.**
Y) Converted data matrix V, expanded to account for the multiplicity of phosphorylations. Data were log2 transformed and normalized. **Human melanoma.**
Z) Scores from inferred kinase activity (INKA) analysis. **Human melanoma.**

Legend supplementary Table 2 (separate Excel file). MaxQuant match between runs option was enabled only for all samples of the same isolation group (MBR-off between urea and RNAB samples).

- Sample overview.
- Raw file overview.

A1) Shortend MaxQuant output after exclusion of reverse hits, contaminants and zero-sum rows. Basis for determination of phosphosite numbers and missing values. **U2OS cells urea.**

A2) Shortend MaxQuant output after exclusion of reverse hits, contaminants and zero-sum rows. Basis for determination of phosphosite numbers and missing values. **U2OS cells RNAB.**

B) Samplewise determined number of all class phosphosites, missing values and their percentages. Based on A1 & A2. **U2OS cells.**

C) Samplewise determined number of class 1 phosphosites, missing values and their percentages. Based on A1 & A2. **U2OS cells.**

D1) Converted data matrix A1, expanded to account for the multiplicity of phosphorylations. Data were log2 transformed and normalized. **U2OS cells urea.**

D2) Converted data matrix A2, expanded to account for the multiplicity of phosphorylations. Data were log2 transformed and normalized. **U2OS cells RNAB.**

E1) Scores from inferred kinase activity (INKA) analysis. **U2OS cells urea.**

E2) Scores from inferred kinase activity (INKA) analysis. **U2OS cells RNAB.**

F) Phosphosite specific signature analysis (PTM-SEA) result for comparison of untreated and irradiated **urea lysed U2OS cells**.

G) Phosphosite specific signature analysis (PTM-SEA) result for comparison of untreated and irradiated **RNAB lysed U2OS cells.**

H1) Shortend MaxQuant output after exclusion of reverse hits, contaminants and zero-sum rows. Basis for determination of phosphosite numbers and missing values. **Mouse liver urea.**

H2) Shortend MaxQuant output after exclusion of reverse hits, contaminants and zero-sum rows. Basis for determination of phosphosite numbers and missing values. **Mouse liver RNAB.**

I) Samplewise determined number of all class phosphosites, missing values and their percentages. Based on H1 & H2. **Mouse liver.**

J) Samplewise determined number of class 1 phosphosites, missing values and their percentages. Based on H1 & H2. **Mouse liver.**

K1) Converted data matrix H1, expanded to account for the multiplicity of phosphorylations. Data were log2 transformed and normalized. **Mouse liver urea.**

K2) Converted data matrix H2, expanded to account for the multiplicity of phosphorylations. Data were log2 transformed and normalized. **Mouse liver RNAB.**

L1) Shortend MaxQuant output after exclusion of reverse hits, contaminants and zero-sum rows. Basis for determination of phosphosite numbers and missing values. **Human liver urea.**

L2) Shortend MaxQuant output after exclusion of reverse hits, contaminants and zero-sum rows. Basis for determination of phosphosite numbers and missing values. **Human liver RNAB.**

M) Samplewise determined number of all class phosphosites, missing values and their percentages. Based on L1 & L2. **Human liver.**

N) Samplewise determined number of class 1 phosphosites, missing values and their percentages. Based on L1 & L2. **Human liver.**

O1) Converted data matrix L1, expanded to account for the multiplicity of phosphorylations. Data were log2 transformed and normalized. **Human liver urea.**

O2) Converted data matrix L2, expanded to account for the multiplicity of phosphorylations. Data were log2 transformed and normalized. **Human liver RNAB.**

P1) Scores from inferred kinase activity (INKA) analysis. **Human liver urea.**

P2) Scores from inferred kinase activity (INKA) analysis. **Human liver RNAB.**

Q1) Shortend MaxQuant output after exclusion of reverse hits, contaminants and zero-sum rows. Basis for determination of phosphosite numbers and missing values. **Human HCC urea.**

Q2) Shortend MaxQuant output after exclusion of reverse hits, contaminants and zero-sum rows. Basis for determination of phosphosite numbers and missing values. **Human HCC RNAB.**

R) Samplewise determined number of all class phosphosites, missing values and their percentages. Based on Q1 & Q2**. Human HCC.**

S) Samplewise determined number of class 1 phosphosites, missing values and their percentages. Based on Q1 & Q2. **Human HCC.**

T1) Converted data matrix Q1, expanded to account for the multiplicity of phosphorylations. Data were log2 transformed and normalized. **Human HCC urea.**

T2) Converted data matrix Q2, expanded to account for the multiplicity of phosphorylations. Data were log2 transformed and normalized. **Human HCC RNAB.**

U1) Scores from inferred kinase activity (INKA) analysis. **Human HCC urea.**

U2) Scores from inferred kinase activity (INKA) analysis. **Human HCC RNAB.**
V1) Shortend MaxQuant output after exclusion of reverse hits, contaminants and zero-sum rows. Basis for determination of phosphosite numbers and missing values. **Human melanoma urea**.

V2) Shortend MaxQuant output after exclusion of reverse hits, contaminants and zero-sum rows. Basis for determination of phosphosite numbers and missing values. **Human melanoma RNAB.**
W) Samplewise determined number of all class phosphosites, missing values and their percentages. Based on V1 & V2. **Human Melanoma.**
X) Samplewise determined number of class 1 phosphosites, missing values and their percentages. Based on V1 & V2. **Human melanoma.**
Y1) Converted data matrix V1, expanded to account for the multiplicity of phosphorylations. Data were log2 transformed and normalized. **Human melanoma urea.**
Y2) Converted data matrix V2, expanded to account for the multiplicity of phosphorylations. Data were log2 transformed and normalized. **Human melanoma RNAB.**
Z1) Scores from inferred kinase activity (INKA) analysis. **Human melanoma urea.**
Z2) Scores from inferred kinase activity (INKA) analysis. **Human melanoma RNAB.**
AA) GO analysis BP for urea unique gene names. **U2OS cells.**
AB) GO analysis BP for RNAB unique gene names. **U2OS cells.**
AC) GO analysis BP for urea unique gene names. **Mouse liver.**
AD) GO analysis BP for RNAB unique gene names. **Mouse liver.**
AE) GO analysis BP for urea unique gene names. **Human liver.**
AF) GO analysis BP for RNAB unique gene names. **Human liver.**
AG) GO analysis BP for urea unique gene names. **Human HCC.**
AH) GO analysis BP for RNAB unique gene names. **Human HCC.**
AI) GO analysis BP for urea unique gene names. **Human melanoma.**